

Isothermal Compressed Air Energy Storage (I-CAES)

A Master's Thesis submitted for the degree of
“Master of Science”

supervised by
Univ. Prof. Dr. Dipl.-Ing. Reinhard HAAS

Alaeldin Mohamed

01168323

Vienna, 08.10.2018

Affidavit

I, **ALAEELDIN MOHAMED**, hereby declare

1. that I am the sole author of the present Master's Thesis, "ISOTHERMAL COMPRESSED AIR ENERGY STORAGE (I-CAES)", 88 pages, bound, and that I have not used any source or tool other than those referenced or any other illicit aid or tool, and
2. that I have not prior to this date submitted this Master's Thesis as an examination paper in any form in Austria or abroad.

Vienna, 08.10.2018

Signature

Acknowledgments

I would like to express my sincere gratitude and appreciation to my thesis supervisor Univ. Prof. Dipl. Ing. Dr. Reinhard Haas for his support and guidance throughout my master thesis journey and during the master program.

I would also like to thank the program manager MMag. Elisabeth Haslinger, my colleagues, and all the staff of the RES master program for making the past two years some of the best moments of my life THANK YOU!!!

Last but not least, I would like to thank my family for all the support and motivation they provided me during my journey in this master program.

“If you want to talk about grid resiliency, energy storage is part of that conversation. If you want to talk about load modulation, demand response, storage is a part of that conversation”.

*Matt Roberts
Vice President – Energy Storage Association*

Abstract

Nowadays, production of electricity and heat from Renewable Energy Sources (RES) is increasing rapidly but, the mismatch of energy generation and consumption is an obstacle for the further development of renewable energy systems which makes depending only in clean energy is not possible, which leads to continuous consumption of fossil fuel and increases in GHG emissions. Energy Storage Systems (ESS) are tackling this problem. In addition, they bring other benefits such as the possibility to sell electricity when prices are high and avoid the cost of backup systems. For over one hundred years, ESS have developed continuously to improve the overall performance of the energy market. In rural areas for developing countries where there is no access to electricity, ESS are critical for off-grid application for renewable energy to achieve poverty reduction and improve living conditions. Compressed Air Energy Storage (CAES) is one of the fastest developing storage technologies able to support utility-scale applications. Small-scale applications are currently under development, and a breakthrough is expected soon.

The paper examines the technological and economic feasibility of the Isothermal Compressed Air Energy Storage (I-CAES) technology. The I-CAES technology captures the heat generated by the compression of air and reuses it during the expansion phase, creating a highly efficient storage system, cost-effective and with low environmental impact. The approach of this paper is to study the traditional CAES, i.e., Diabatic and Adiabatic CAES systems and compare it to the I-CAES system to see what the I-CAES system can offer technologically and economically to the existing technology for both large and small-scale applications.

Keywords: *Isothermal, Compressed Air Energy Storage, Renewable Energy, Economic Feasibility, Technological appraisal*

Table of Contents

Acknowledgments	I
Abstract	III
1. Introduction	1
1.1. Motivation	1
1.2. Core Objectives & Main Research Questions	2
1.3. Review of the Literature	3
1.4. Structure of the Master Thesis	4
2. Background Information	5
2.1. Overview of Energy Storage	5
2.2. General Description of CAES	12
2.3. Different CAES Technologies	13
2.4. State-of-the-Art – CAES	18
2.5. Thermodynamics Definitions Governing I-CAES	23
2.6. Current Development of the I-CAES technology	29
3. Method of Approach	34
4. Technological Description	37
4.1. Efficiency of I-CAES	37
4.2. Heat Transfer Based on Water Spray for I-CAES	41
4.3. I-CAES / Off-Grid System	43
4.4. I-CAES / Wind Power	47
5. Economic Evaluation	54
5.1. Levelized Cost of Electricity (LCOE)	54
5.2. CAES Cost	56
5.3. Case Studies	57
5.4. Economic of I-CAES	68
6. Conclusion	71
Bibliography	72
Abbreviation	76
List of Figures	78
List of Tables	81

1. Introduction

1.1. Motivation

During our country module with the master class in Germany, my interest in ESS had increased when I had the chance to learn more about Energiewende. It is a plan from Germany for a long-term structural change in energy systems to achieve their targets for 2020 and 2030. Currently, the plan is facing some difficulties to meet its objective for the reason that, Germany implemented large RE system projects at one time especially off-shore wind turbines. These projects are generating a large amount of energy mostly at the time when demand is low. For this reason, a large share from the power generated is not used but rather given to another country with a negative price. The 4th Energiewende Monitoring Report said that Germany has to lower its energy consumption, increase the energy efficiency and expand the power grid (The Federal Ministry for Economic Affairs and Energy, 2015: 16-17). Knowing that ESS have the potential to support achieving these goals gave me a strong motive to learn more about it. Besides, I had the opportunity to do an internship at the United Nations Industrial Development Organization (UNIDO). That helped me to gain a sense of the importance of enhancing the use of renewable sources for productive use. This enhancement is critical to mitigating Greenhouse gasses (GHGs) emissions to facilitate achieving international targets (e.g., the Paris agreement). ESS can play a major role to improve the efficiency of RE systems leading to a reduction in cost and facilitating access to affordable and sustainable energy, especially in developing countries.

Moreover, I was inspired by a young entrepreneur, Danielle Fong. She is the co-founder and Chief Scientist of LightSail Energy. The company was founded in 2009 to develop a new form of CAES. The system stores energy in the form of compressed air using the isothermal process. Danielle also focused on how to eliminate the geographical constraint associated with the technology (i.e. using underground caverns as a reservoir for the compressed air).

Those mentioned above along with the global trend towards a green world motivated me to do my thesis on I-CAES technology to examine its capability to be an efficient and cost-effective storage system to support large and small-scale applications to help the deployment of RE systems.

1.2. Core Objectives & Main Research Questions

The focus of this paper is on the I-CAES technology. The following core objectives of this thesis and the research questions were chosen to facilitate understanding the technology.

(i) an overview of ESS and its importance for the deployment of RE systems, **(ii)** an overall idea about traditional CAES systems and the difference between them, **(iii)** study the thermodynamics behind the I-CAES system to get a better understanding of the technique used in the I-CAES technology to improve the system efficiency, **(iv)** review the current development of the I-CAES system to get a better sense of the maturity of the technology, **(v)** examine the technological feasibility of the I-CAES system (i.e. the efficiency of the system and the effectiveness of the method used for transferring heat), and its ability to support off-grid and large-scale applications, **(vi)** assessing the economic feasibility of traditional CAES when integrated within large-scale RE systems in order to examine the economic feasibility and improvements the I-CAES system can add to the traditional CAES systems, and **(vii)** study the financial difference between small and large scale I-CAES systems.

Questions to be addressed:

- What are the concepts of I-CAES and traditional CAES systems, i.e., Diabatic, Adiabatic?
- What is the state-of-the-art of the CAES system?
- What is the current development of CAES technology?
- What are the thermodynamic definitions governing the I-CAES?
- How to calculate the efficiency of the I-CAES system?
- What are the methods used to achieve an isothermal process, i.e., isothermal compression and expansion?
- What contribution can the I-CAES technology offer to support small-scale off-grid and large-scale RE applications?
- How can the I-CAES system affect the economic situation of the CAES technology?
- What are the economical differences between large and small I-CAES systems?
- What are the economical disadvantages associated with the use of I-CAES technology?
- What is the future direction for the I-CAES technology?

1.3. Review of the Literature

The International Energy Agency (IEA) made it very clear in their report “Contribution of Renewable Energy to Energy Security” (IEA, 2007: 5) that, reaching the goal of a sustainable energy system can only be achieved by RES supported by ESS. Only then we can improve the security of the energy supply, ensure the safety of the grid, and improve the efficiency of RE systems. ESS support different applications depending on its characteristics. These applications can be divided into large and small-scale applications. According to the Institute of Engineering Thermophysics, Chinese Academy of Sciences (Chen H. et al., 2013: 102), Beside Pumped Hydro Storage (PHS), CAES is the only large-scale storage system that is commercially available. Though, the traditional CAES technology (i.e., Diabatic CAES) have big disadvantages which they are, (1) the low round-trip efficiency where the heat generated by the compression process is wasted to the environment and contribute to more GHGs emission and (2) the dependency on fossil fuel for the expansion process that increases the cost of the system. A joint research published by the Molecular Diversity Preservation International and Multidisciplinary Digital Publishing Institute (MDPI) (Wang J. et al., 2017: 22). Therein, they conclude that the utilization of the heat generated from the compression process can avoid using fossil fuel and improve the overall efficiency of the system. LightSail Energy Company founded by Danielle Fong came up with a new method to utilize the heat generated from the compression process (Taranovich S., 2012). The method is to capture the heat and store it before it lost using water. Then, the stored heat is reused during the expansion process. They also came up with a storage idea that eliminates the geographic constraint. Also, SustainX company which is another company working on I-CAES said, storing the captured heat eliminates the need for a gas combustion turbine and improves efficiency (SustainX, 2012). In 2014, Sean Wright from the Electric Power Research Institute (EPRI) presented in a demonstration project webcast a comparison for two I-CAES system leading vendors, SustainX and LightSail Energy (EPRI, 2015: 1-5). Although many details of LightSail Energy technology have not been made public, the comparison illuminates many of the opportunities and challenges facing this role of the energy storage industry. Moreover, a research on the development trend of compressed air energy storage published by Informa UK Limited, trading as Taylor & Francis Group (Wang J. et al., 2017: 434) conclude that, to reduce the cost of CAES system, it has to be utterly renewable because a lot of the cost goes to the generation process.

1.4. Structure of the Master Thesis

Chapter 1: Explain the need for ESS technology and the supporting characteristics for some of the applications.

Chapter 2: Background information, i.e. a general description of the CAES technologies and the different methods used to operate the technology. Also, the study of the State-of-the-Art of the technology of existing CAES plants and their operating conditions. In addition, addressing the thermodynamic definitions governing the technology to examine how the technology converts electricity into mechanical work and again into electricity and how to deal with the heat. The last thing in this chapter is, having a sight on the current development status of the technology and companies working on it.

Chapter 3: Analyzing the technical and technological aspects of the CAES technology in general and the I-CAES in specific. Moreover, study the method of water spraying to absorb and store heat to obtain an isothermal process. Also, an assessment of I-CAES to support off-grid applications and large-scale RE.

Chapter 4: Economic evaluation of the CAES system and examination of the economic potential of I-CAES to reduce cost and increase.

Chapter 5: Conclusion and results

2. Background Information

2.1. Overview of Energy Storage

ESS are essential when talking about RE Systems because it gives us a tool to match production with consumption when producing energy from intermittent sources such as solar and wind. In recent decades, RES has increased dramatically mainly wind and solar systems resulting in the reduction of Greenhouse gasses (GHGs). According to the statistical review of world energy by the BP company in June 2017 (*bp, 2017: 2*), RE Systems (excluding hydro) grew by 14.1% in 2016 of which more than 50% is wind, and 18% is solar. Though, when comparing the installed capacity with the energy production to calculate the load factor, we realize that there is an enormous difference between what the systems produce and their generation capacity. The load factor for a wind plant is low as 22%, and for solar it is 12% (*Stoppato A. & Benato A., 2017: 2*). This difference is due to the dependency of RE systems on intermittent power sources where the variability of the sun and wind throughout the year makes the plants operate for a limited number of hours per year. RE plants have changed the structure of the electricity network in the sense that instead of few large-scale production plants. Nowadays small, medium and large RE plants are spread all over the country. These changes in the electricity network affected the power grid so that more transformers, power lines and protection systems are needed. As mentioned before, the rapid increase in RE facilities created problems such as the balance between supply and demand, frequency and voltage regulation and overloading the power lines. ESS technologies can help to control our supply systems and insure the safety of the grid. **Figure 1** summarize the problems with RE installations and possible solution for them (i.e., the use of ESS). ESS technologies vary in their characteristics in which, there is no specific storage system valid for all type of applications. For instance, batteries cannot endure high cycling rates therefore, they are not applicable for grid applications. In addition, the amount of the power and energy density the ESS has determines the size of the technology. **Table 1** below list some of the typical ESS applications and the key characteristics to support them and **Table 2** shows the values for some of ESS attributes for different EES technologies. Also, **Figure 2** shows different ESS technologies that are categorized to support different proposed applications according to its power rating and charge/discharge timescale.

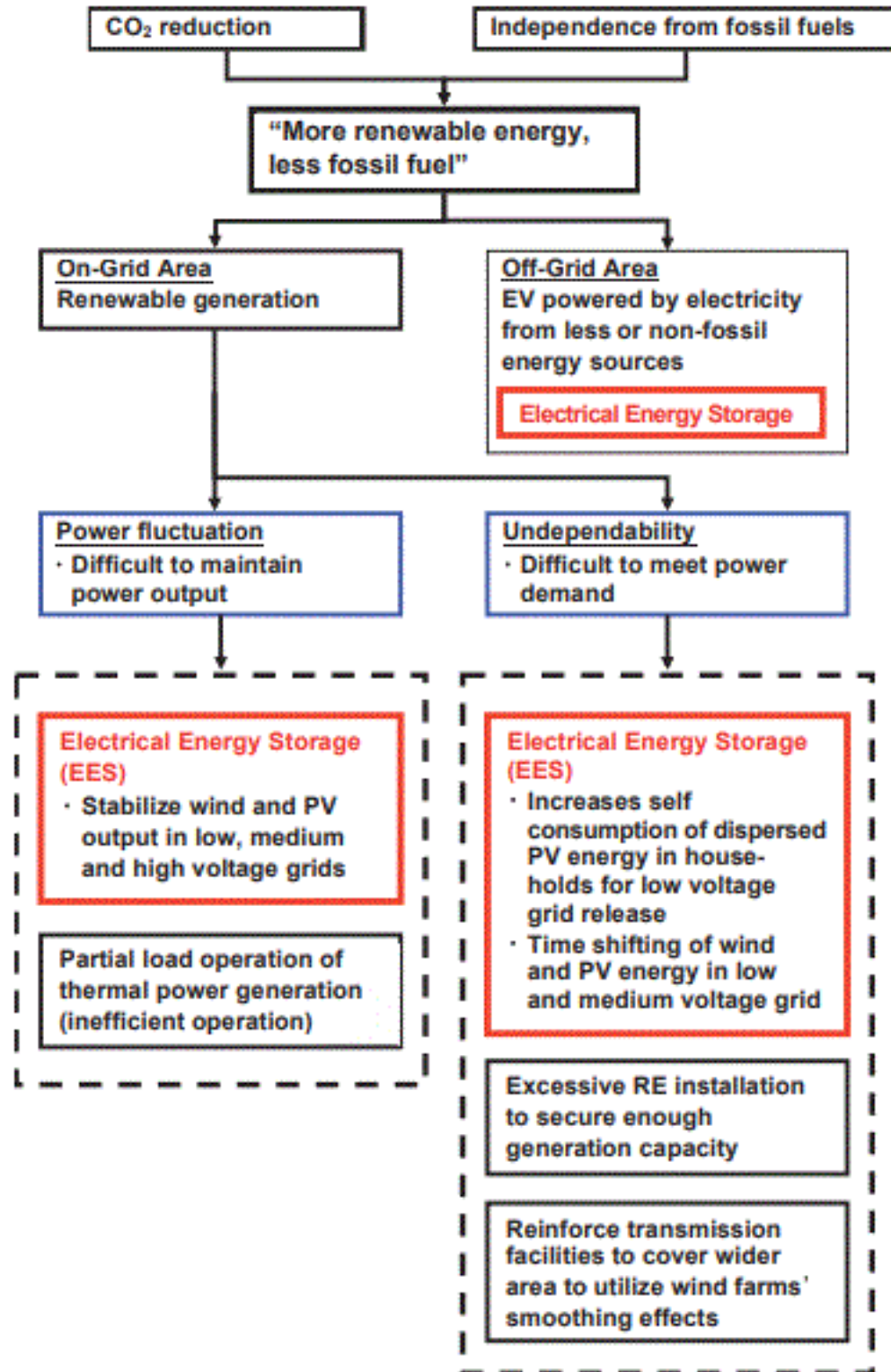


Figure 1: Problems with RE installation and possible solutions (Source: IEC, 2011: 12)

Table 1: Characteristics of ESSs for typical applications in the energy system (Source: IEA, 2014: 9)

Application	Size (MW)	Discharge duration	Cycles (typical)	Response time
Seasonal storage	500 to 2 000	Days to months	1 - 5 per year	day
Arbitrage	100 to 2 000	8 hours to 24 hours	0.25 - 1 per day	>1 hour
Frequency regulation	1 to 2 000	1 minute to 15 minutes	20 - 40 per day	1min
Voltage support	1 to 40	1 second to 1 minute	10 - 100 per day	millisecond second
Black start	0.1 to 400	1 hour to 4 hours	< 1 per year	<1 hour
Off-grid	0.001 to 0.01	3 hours to 5 hours	0.75 - 1.5 per day	<1hour
Spinning reserve	10 to 2 000	15 minutes to 2 hours	0.5 to 2 per day	<15 min
Non-spinning reserve	10 to 2 000	15 minutes to 2 hours	0.5 to 2 per day	<15 min
Combined heat and	1 to 5	Minutes to hours	1 to 10 per day	< 15 min
Waste heat utilization	1 to 10	1 hour to 1 day	1 to 20 per day	< 10 min

Table 2: Main characteristics of ESSs (Source: Wang J. et al., 2017: 2)

Technology	Energy density (Wh/L)	Power rating (MW)	Lifetime (year)	Discharge time	Cycling time (cycles)	Maturity
PHS	0.5 – 2	30 – 5000	40 – 60	1 – 24 Hrs+	10,000 – 30,000	Mature
Flywheel	20 – 80	0.1 – 20	15 – 20	Sec – 15 Min	20,000	Early com
CAES	2 – 6	≥300	20 – 40	≥30 Min	8000 – 12,000	Early com
SMES	0.2 – 6	0.1 – 10	20 – 30	1 – 24 Hrs+	10,000+	Demo/Early com
Solar fuel Hydrogen	500 – 10,000	0 – 10	-	Sec – 24 Hrs+	1000+	Developing
Li-ion	150 – 500	0 – 100	5 – 15	Min – Hrs	1000 – 10,000	Demo
Lead-acid	50 – 90	0 – 40	5 – 15	Sec - Hrs	5000 – 10000	Mature
Hydrogen fuel cell	500 – 3000	0 – 50	5 – 20	Sec – 24 Hrs+	1000+	Developing

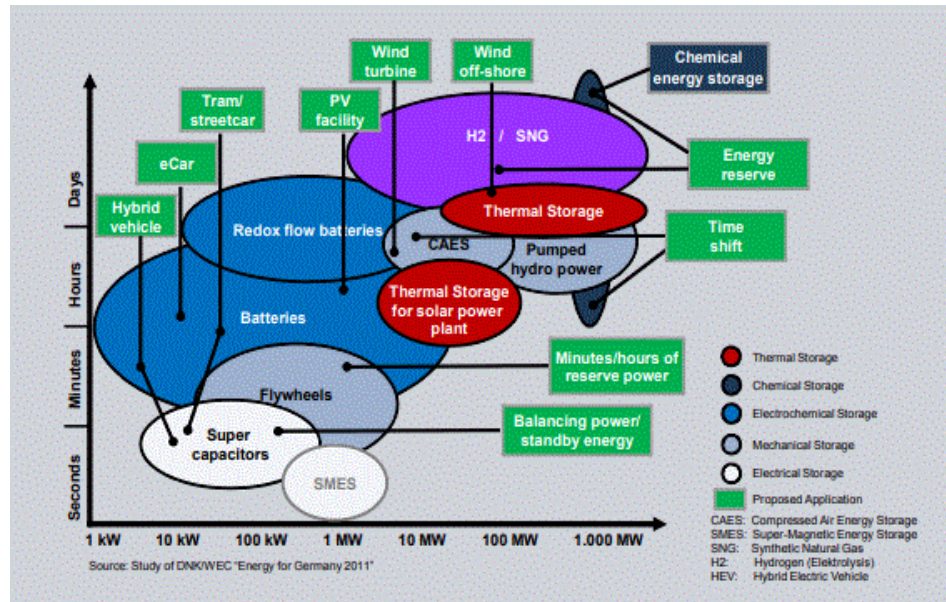


Figure 2: Energy storage technologies categorized according to available power and typical charge/discharge timescale, including several proposed applications (Source: Muñoz S. A. et al., 2016: 28)

The energy and power density determines the size of an ESS (Muñoz S. A. et al., 2016: 24). Figure 3 shows a comparison of energy and power density for superior ESS technologies.

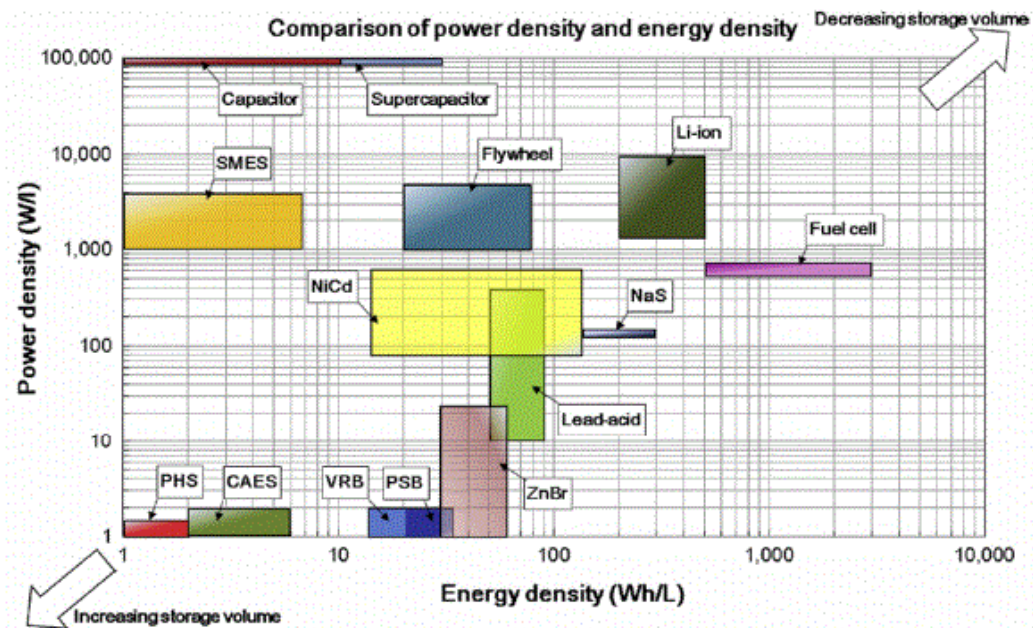


Figure 3: Comparison of power density and energy density for different ESS technologies (Source: Muñoz S. A. et al., 2016: 24)

The power rating and the discharge time of an ESS can determine the application it can effectively support. **Table 3** shows the category application, and its specifications and **Figure 4** shows the category application and ESS that support them.

Table 3: Application category and its specifications (Source: Susan M. et al., 2003: 11)

Application Category	Discharge power range	Discharge time range	Stored Energy Range	Representative Applications
Bulk Energy Storage	10 – 1000 MW	1 – 8 hours	10 – 8000 MWh	Load leveling, spinning reserve
Distributed Generation	100 – 2000 MW	0.5 – 4 hours	50 – 8000 MWh	Peak shaving, transmission deferral
Power Quality	0.1 – 2 MW	1 – 30 seconds	0.028 – 16.67 MWh	End-use power quality and reliability

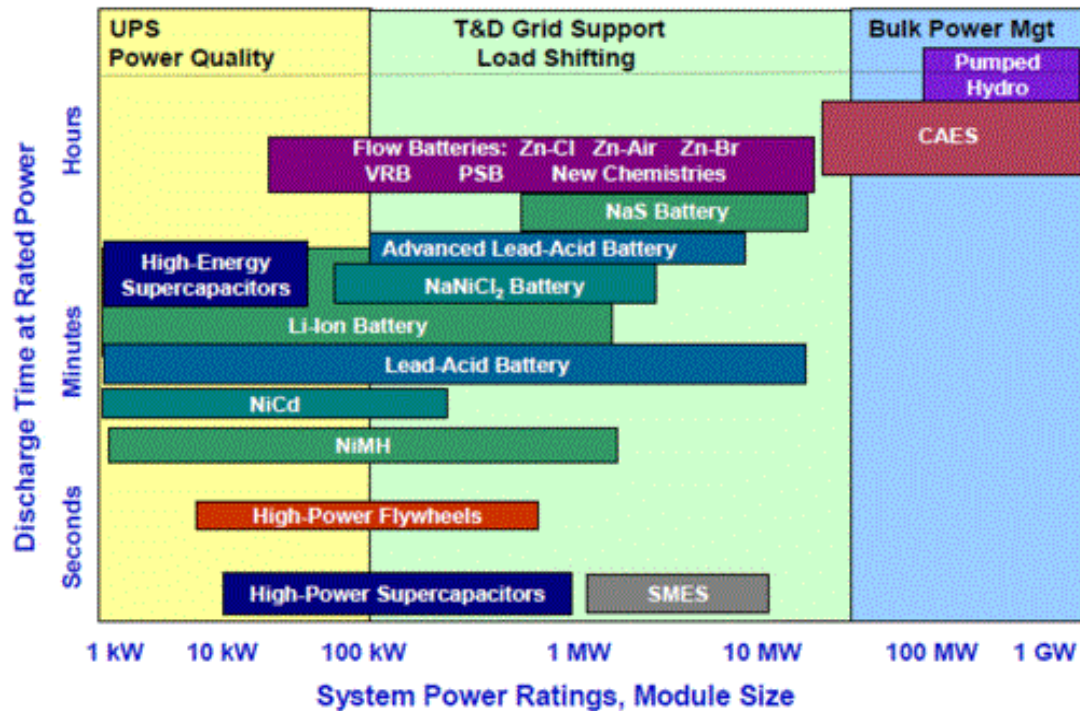


Figure 4: ESS technologies categorized according to the type of application areas based on power rating and rated energy capacity (Source: Muñoz S. A. et al., 2016: 23)

Sometimes, more than one ESS technology is suitable for one specific application that is why an economic appraisal is vital when choosing an ESS to support an application.

Figure 5 shows the power and energy costs of ESS technologies.

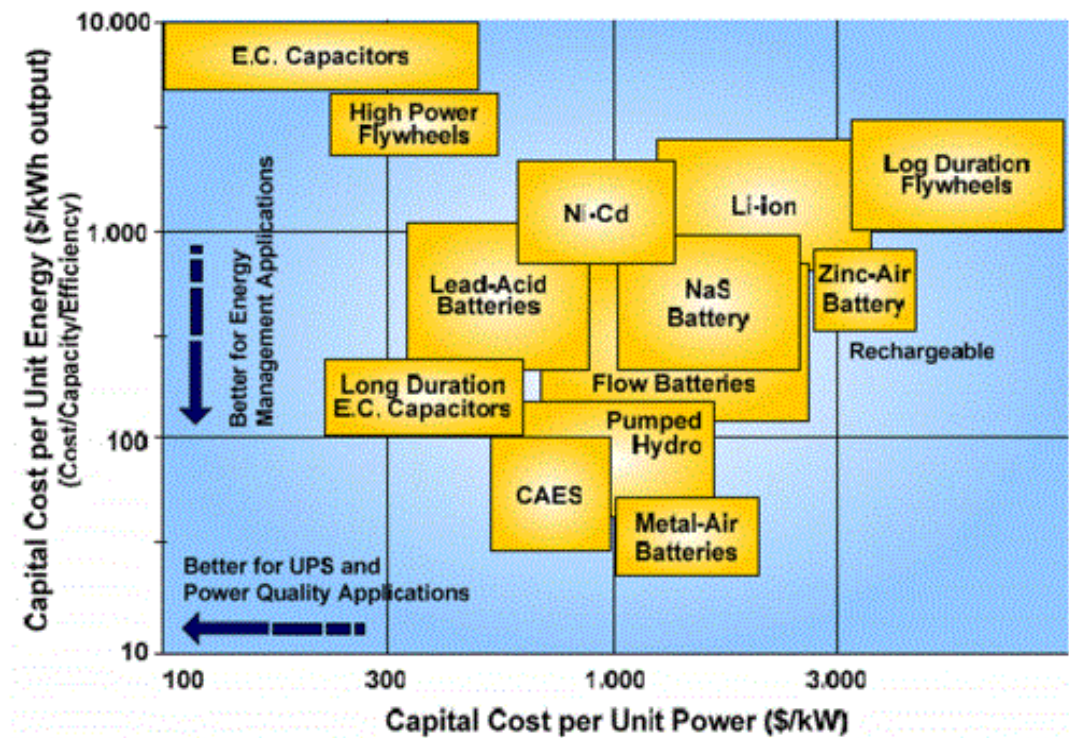


Figure 5: Investment cost of ESS technologies (Source: Muñoz S. A. et al., 2016: 25)

Based on ESS energy storage capacity, it can be categorized as long-term and short-term ESS. Some applications require long-term ESS like the seasonal storage application, and some require short-term storage systems like the frequency regulation application (IEA, 2014: 21). ESS that supports short-term applications usually have high cycle lives and power density, but low energy density. On the other hand, ESS that supports long-term applications must have a high energy capacity (IEA, 2014: 21). The discharge time of an ESS technology determines whether it can support long-term or short-term applications. **Table 4** shows some of ESS that supports long-term applications and ESS that support short-term applications.

Table 4: ESS technologies for long and short-term applications (Source: IEA, 2014: 18)

<i>Long-term</i>	<i>Short-term</i>
<i>PSH</i>	<i>Flywheels</i>
<i>UTES</i>	<i>Super capacitors</i>
<i>CAES</i>	<i>Superconducting magnetic energy storage (SMES)</i>
<i>Chemical hydrogen storage</i>	<i>Batteries</i>

2.2. General Description of CAES

CAES is a mechanical storage system based on thermodynamic cycles. A simple illustration for the technology that people are familiar with is, pumping up car tires. The person pumping the tires is putting energy in the form of compressed air and stores it inside the tires. Once the person wants to recover the energy stored in the tire, the person releases the compressed air from the tires into a container. This illustration has almost all of the CAES's processes, the only part missing is, how to manage the thermal energy generated from the process. Generally, CAES uses the surplus electricity during low power demand to drive a compressor to inject air into storage containers. The storage containers could be underground caverns for large-scale systems with a pressure between 48 – 66 bars or an overground air tanks for small-scale systems with a pressure up to 300 bar (Luo X. & Wang J., 2013: 22-25). During high power demand, the compressed air is released from the storage facility and reheated using either an external heat source, e.g. from the combustion of fossil fuels or using the heat recovered from the compression process. In the expansion phase, the temperature falls because work is extracted from the compressed air to operate a motor/turbine and generate electricity to be sent back to the grid.

CAES uses a wide variety of technologies, i.e., compression machinery, expansion machinery, a heat exchanger, and several compressed air and thermal storage options (Garvey S. D. & Pimm A., 2016: 102). There are different CAES processes. If the heat used in the expansion phase was brought from an external source (combustion of fossil fuels) then, the process is called Diabatic Compressed Air Energy Storage (D-CAES). D-CAES system is considered a hybrid system composed of an energy storage system and an energy generation system. There are two other CAES processes. These processes are called Adiabatic and Isothermal Compressed Air Energy Storage (A-CAES) & (I-CAES). They store the heat generated during the compression phase and reuse it during the expansion phase to minimize the energy loss.

2.3. Different CAES Technologies

➤ D-CAES System

D-CAES is considered the least efficient process among CAES processes, for the reason that all the heat generated during the compression process is removed via a cooling system and gets lost. That means a tremendous amount of energy is completely wasted. The compressed air is stored in underground salt caverns; these caverns are at hundreds on meters depth (between 500 *m* – 800 *m*) and under a pressure of approximately 100 bar (EASE, 2018). When there is demand, the compressed air is released for the expansion phase and heat is added to it via combustion of fossil fuel to drive the turbine. **Figure 6** represents the most straightforward D-CAES system and **Table 5** present the key performance data of a typical D-CAES plant.

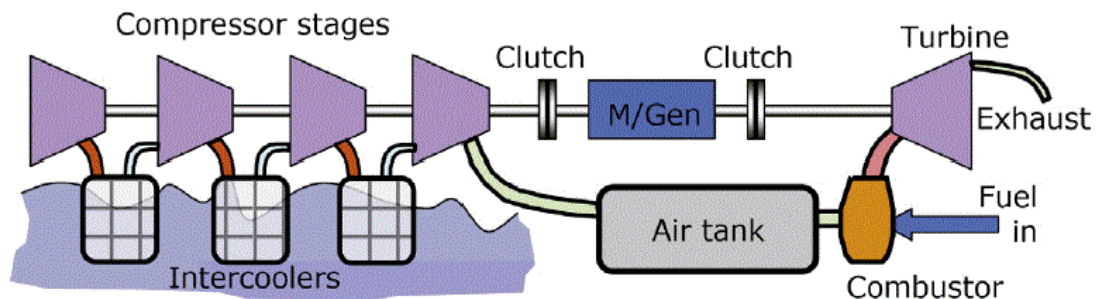


Figure 6: D-CAES system (Source: Garvey S. D. & Pimm A., 2016: 103)

Figure 7 shows a developed D-CAES system that has enhanced the round trip efficiency by adding a recuperator to receive the heat from the exhaust and transfer it to the compressed air before the expansion stage. Another way to enhance the efficiency is by adding a recuperator and more expansion stages so that more work is extracted (**Figure 8**). The process starts by compressing air at ambient temperature in three stages to reach the maximum possible pressure and then expand it, after the first expansion stage the heat is sent to the recuperator to raise the temperature of the pressurized air before the second stage to get more work out of it (Garvey S. D. & Pimm A., 2016: 104). The temperature/pressure plot of the system is shown in **Figure 9**.

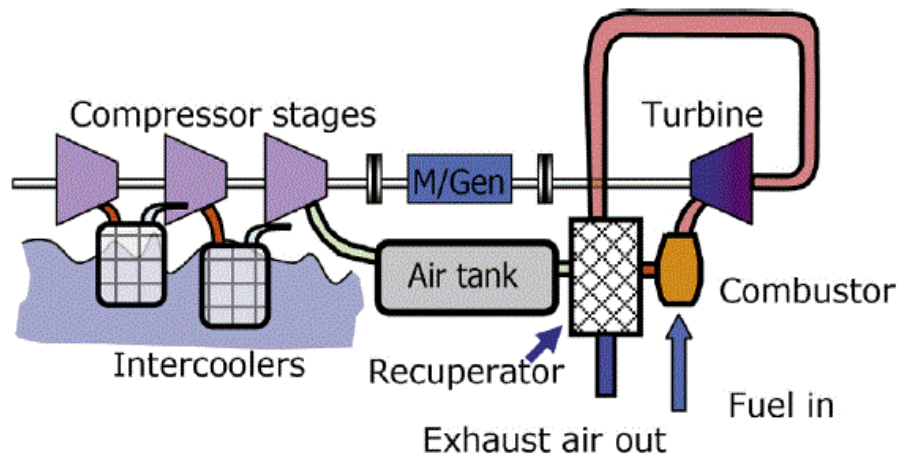


Figure 7: D-CAES system with recuperator (Source: Garvey S. D. & Pimm A., 2016: 103)

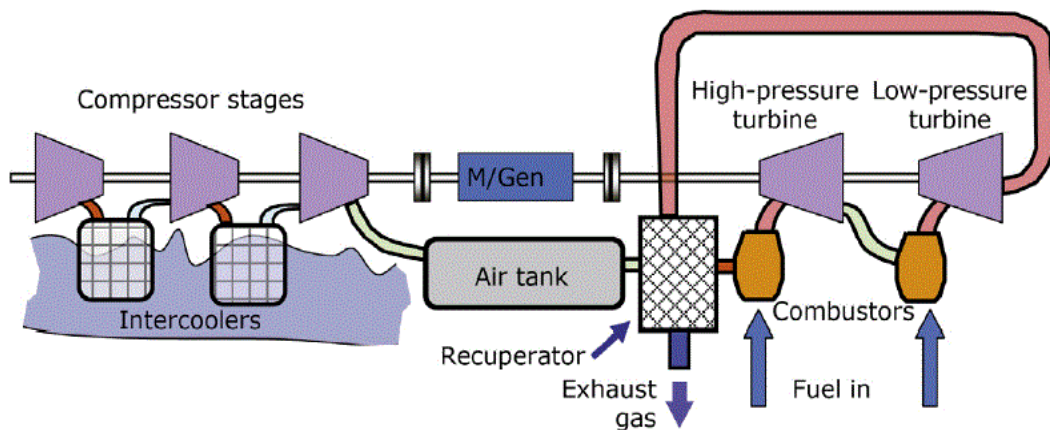


Figure 8: D-CAES system with recuperator and two expansion stages (Source: Garvey S. D. & Pimm A., 2016: 104)

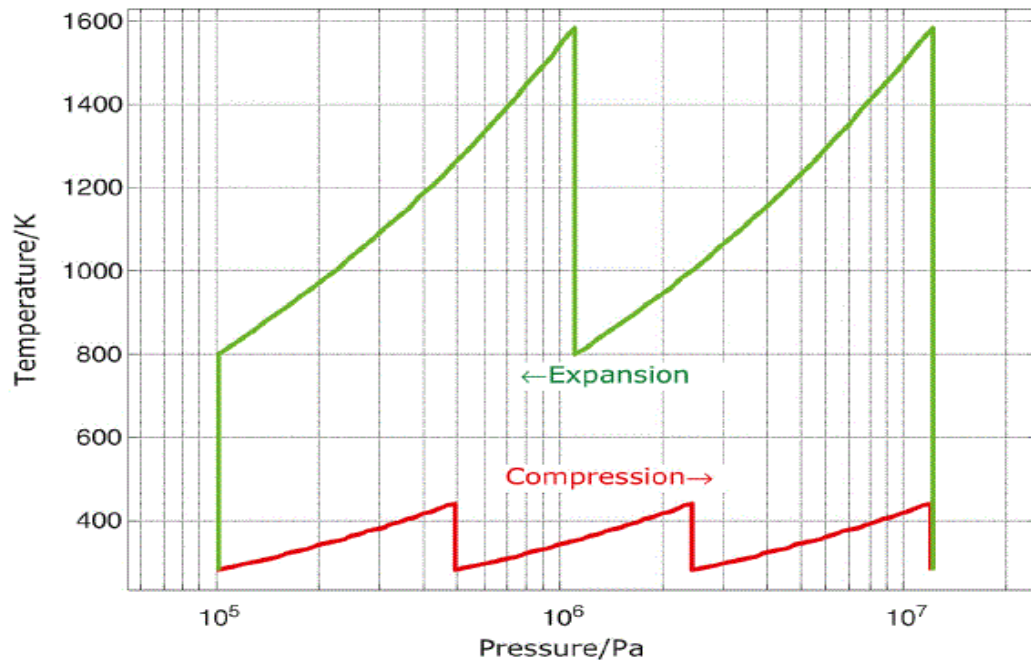


Figure 9: Temperature/Pressure plot of D-CAES with three compression stages and two expansion stages and recuperator (Source: Garvey S. D. & Pimm A., 2016: 104)

Table 5: D-CAES key performance data (Source: EASE, 2018)

Power range	$\cong 100 \text{ MW}$
Energy range	100 MWh – 10 GWh
Discharge time	1 h – 10 h
Life duration	> 30 years
Reaction time	Few mins
Efficiency	$\cong 50\%$
CAPEX: energy	50 – 150 €/kWh
CAPEX: power	400 – 1,200 €/kW

➤ A-CAES System

In A-CAES, thermal energy storage is added to replace external heat sources, i.e., combustion of fossil fuel. A-CAES captures the heat generated by the compression process that reaches 600°C and stores it in Thermal Energy Storage (TES), i.e., reliable materials such as ceramic, concrete or natural rock materials (EASE, 2018). The technology also stores the compressed air in an underground cavern at hundreds of meters of depth and a pressure up to 100 bar (**Figure 10**). In the discharging process, the compressed air is released, and before it goes to the turbine, it passes through the TES to get reheated again without the need for combustion of fossil fuels. In spite of the potential the A-CAES has, it is not yet commercially available. The European Commission Framework Programme has conducted a research in which they reached the final plant design. The plant design has the potential to store 1 *GWh* of energy and drive about 200 *MW* power turbine (EASE, 2018). The construction of such a plant requires a massive investment in which the risk is high because the technology is not mature yet. That is why a demonstration plant is needed but, even a demonstration plant will still need to be in the range of 100 *MW* power so as to be economically feasible (EASE, 2018).

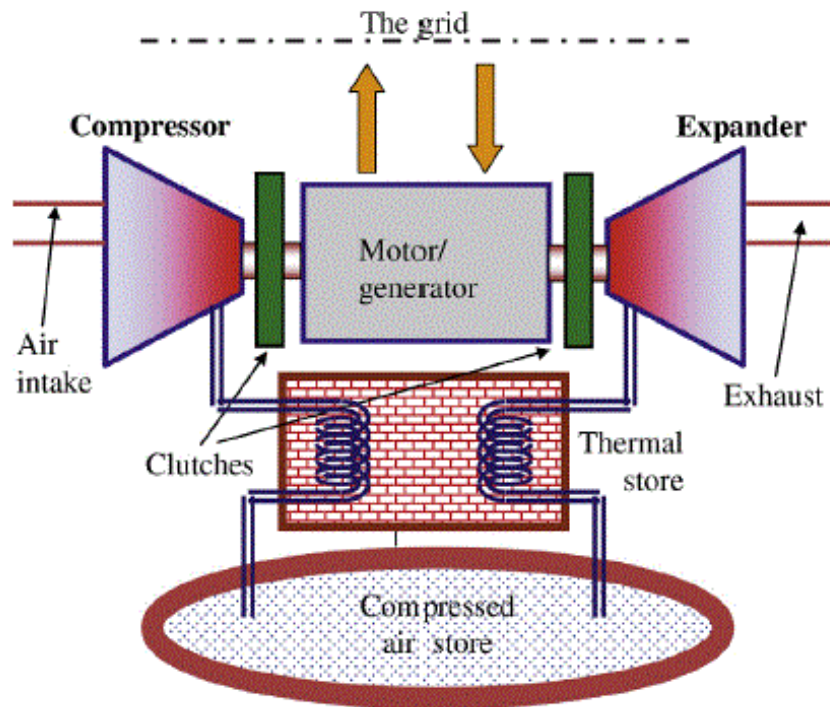


Figure 10: A-CAES with thermal storage (Source: Garvey S. D. & Pimm A., 2016: 106)

Table 6: A-CAES key performance data (**Source: EASE, 2018**)

Power range	$\cong 100 \text{ MW}$
Energy range	100 MWh – 10 GWh
Discharge time	1 h – 10 h
Life duration	> 30 years
Reaction time	Few mins
Efficiency	$\cong 70\%$
CAPEX: power	400 – 1,200 €/kW

➤ I-CAES System

I-CAES is an emerging technology strain to overcome the inefficiency of traditional CAES technologies. I-CAES captures the heat before it is lost and use it to reheat the stored compressed air before the expansion phase, therefore, increasing the overall system efficiency dramatically and reduce the cost (*Wang J. et al., 2017: 12*). The isothermal process maintains a constant temperature by removing heat continuously from the air during the compression process and adding it continuously during the expansion process, therefore, eliminating the need for the combustion of fossil fuel in the D-CAES system and the TES in the A-CAES system.

To maintain a constant temperature throughout the compression and expansion phases; it is essential to transfer heat generated by the compression process at a rapid rate to the compressed air during the expansion process to keep a minimum temperature difference (*Gavery S. D. & Pimm A., 2016: 92*). The speed rate in which heat transfer takes place is proportional to the temperature gradient multiplied by the surface, for this reason, a large surface area is essential to maintain a near-isothermal process (*ESA, 2018*). The technology is still not commercially available, though, few implementation ideas have been proposed that strain to remove the heat generated from the compression process and add it through the expansion process, one approach is to spray fine, dense water droplet within a large surface area to absorb the heat and store it. During the expansion, heat is added through the warm water and the cycle is repeated (*ESA, 2018*).

2.4. State-of-the-Art – CAES

In recent days, two commercial large-scale CAES power plants are running, both of them are D-CAES systems. One in Germany so-called Huntorf and the other one is the McIntosh power plant built in the USA. In addition, a few companies are carrying out a lot of studies and demonstrations for new ideas and technologies to accelerate the growth of CAES technology and make it more feasible to invest and more environmentally friendly.

Table 7: Key features - Huntorf and McIntosh CEAS plants (Source: Wang J. et al., 2017: 10)

	Year	Power (MW)	Energy (MWh)	Pressure (Mpa)	Heat Source	Efficiency (%)
Huntorf	1978	290	580	4.6 – 6.6	Natural Gas	42
McIntosh	1991	110	2860	4.5 – 7.4	Natural Gas	54

➤ Huntorf Power Plant

Huntorf is the world first CAES plant near Huntorf, Germany north-west of. The plant was established in 1978 with a capacity of 290 MW Breman (Boveri & CIE, 1978: 6). The storage system is a Diabatic system and, as mentioned before, D-CAES system is considered as a hybrid system composed of an energy storage system, and a power generation system. In this case, the power generation system is a gas turbine. The plant has two 800 m deep salt underground caverns with a total volume of approximately 300,000 m³ (Boveri & CIE, 1978: 6). The charging process takes 8 hours and, the underground storage pressure at the caverns reaches up to 72 bar (Figure 11).

Figure 12 shows the operating data of the storage system. The compressor compresses air at the rate of 2.5 bar/h during the 8 hours charging duration. The discharging duration is 2 hours with a rate of 10 bar/h. That means, the output pressure from the storage system is 20 bar (Boveri & CIE, 1978: 5).

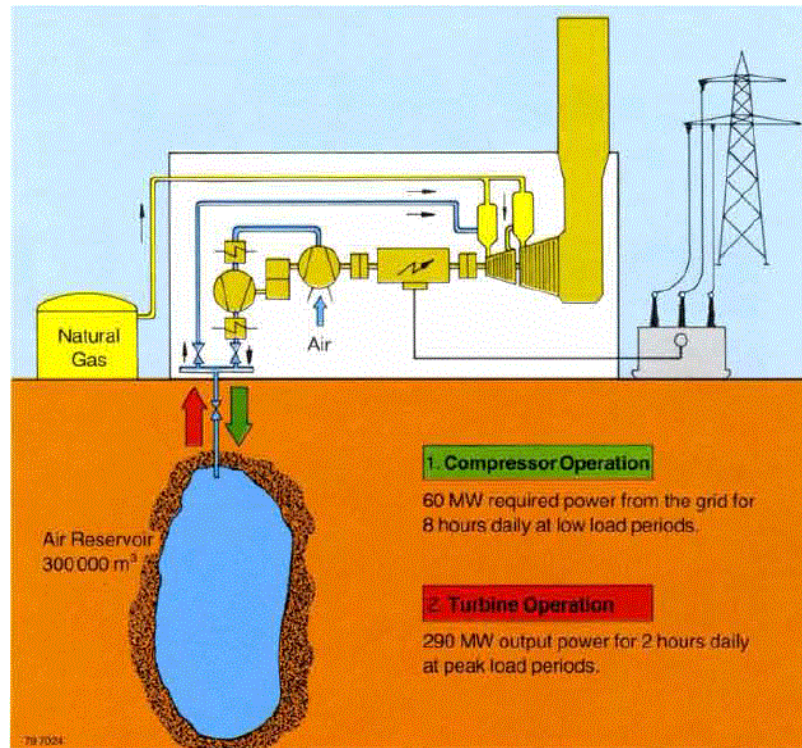


Figure 11: Huntorf Power plant (Source: Boveri & CIE, 1978: 5)

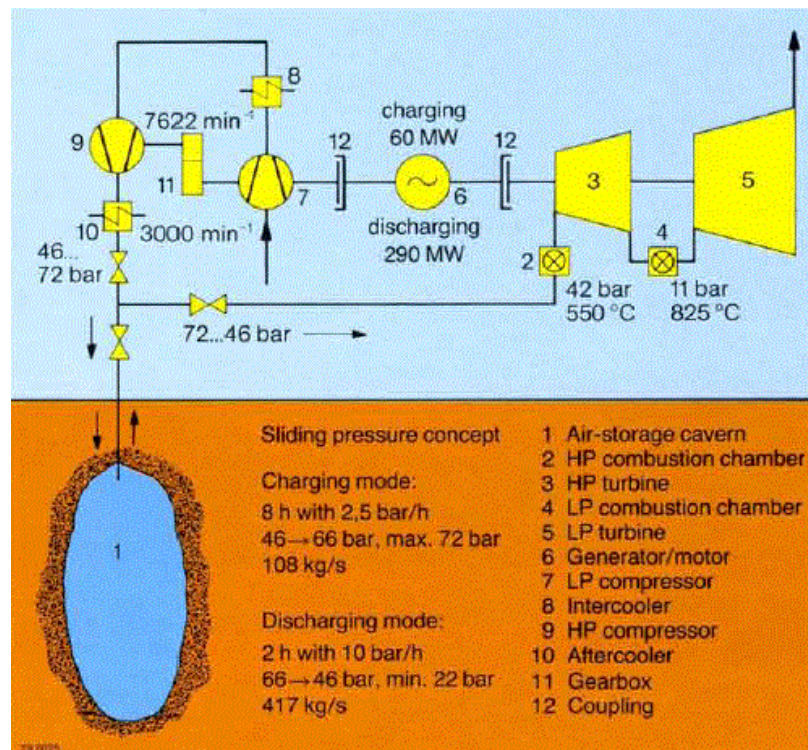


Figure 12: Operating Data of Huntorf Storage System (Source: Boveri & CIE, 1978: 9)

Table 8: Operating conditions for the Huntorf plant (Source: Raju M. & Kumar K. S., 2012: 476)

Operating condition	Value	Unit
Gas turbine		
Rated turbine power	290	MW
Air consumption 417 kg/s	417	kg/s
Inlet pressure HP turbine	42	bar
Inlet temperature HP turbine 550 _C	550	°C
Inlet pressure LP turbine	11	Bar
Inlet temperature LP turbine	825	°C
Fuel	Natural gas	
Compressor		
Airflow rate	108	kg/s
Rated compressor power	60	MW
The temperature aftercooler	50	°C
The pressure at the exit of the aftercooler	46-72	bar
Cavern		
The volume of the cavern storage	300,000	m ³
Cavern operating pressure	46-66	bar
Maximum cavern pressure	72	bar
Maximum discharge rate	10	bar/h
Cavern wall temperature	~50	°C

For the Huntorf power plant to achieve 1 *KWh* output, 0.8 *KWh* of electricity from an external source is needed to be added to 1.6 *KWh* from fossil fuel combustion (Seamus, D. & Pimm, A., 2016: 108).

$$\text{eff}_{\text{Huntorf}} = \frac{1}{0.8 + 1.6} = 41.6\% \quad (1)$$

➤ McIntosh power plant

The McIntosh power plant is another D-CAES system based plant. It was built in Alabama, USA, in 1990 with a capacity of 110 *MW* (Wang J. et al., 2017: 4). The McIntosh power plant can store energy up to 2700 *MWh* and it can operate delivering power up to 26 *h* when fully charged (Wang J. et al., 2017: 4). The plant has salt underground caverns at a depth of 450 *m*, an volume of 538,000 *m*³ and a pressure of 45 – 76 bar (Wang J. et al., 2017: 10).

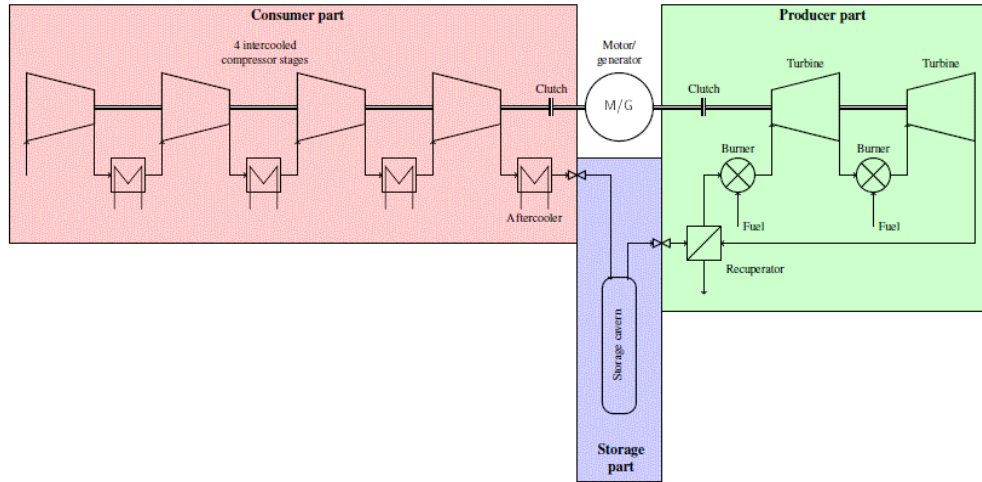


Figure 13: McIntosh power plant (Brian E. & Brix W. M., 2011: 7)

For the McIntosh power plant to achieve 1 *KWh* output, 0.69 *KWh* energy is added from an external source and added to 1.6 *KWh* produced from fossil fuel combustion (Gavery S. D. & Pimm A., 2016: 108).

$$\text{eff}_{\text{McIntosh}} = \frac{1}{0.69 + 1.17} = 53.8\% \quad (2)$$

➤ ADELE Power Plant

In 2008, a study for the first large-scale A-CAES with a 70% system efficiency was presented by RWE and General Electric in Germany by the name ADELE (**Figure 14**) (*RWE Power AG, 2010: 5*). ADELE's concept is to use the experience of the Huntorf plant and improve the system efficiency by using an Adiabatic process, it means, as mentioned before, to store heat generated from the compression process in ceramic materials and restore this heat during the expansion process to heat the compressed air. Therefore, no gas combustion is required (*Raible M., 2016: 4*).

First, Ambient air is compressed to around 70 bar using an electrically driven compressor. During the compression process, heat generated at 600°C (*Wang J., 2017: 16*). The hot air flows through a well-isolated heat accumulator to recover as much energy as possible. The accumulator consists of ceramic materials with a high heat storage capacity. Next, the compressed air flows into an underground salt cavern to be stored at 4°C until it is needed again (*Raible M., 2016: 7*). Whenever the demand for power increases, the compressed air is released from the underground salt cavern and goes through the heat accumulator to raise its temperature. From there, it flows into the turbine to generate electricity to be sent to the grid.

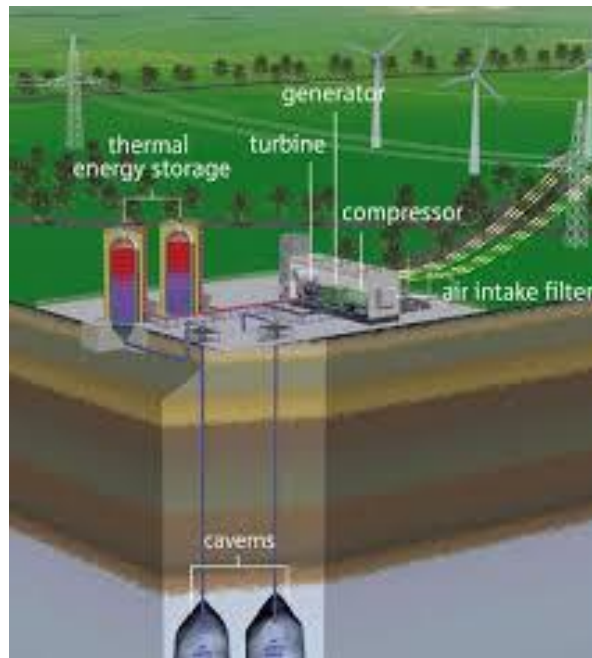


Figure 14: A-CAES plant - ADELE (Source: RWE Power AG, 2010: 5)

2.5. Thermodynamics Definitions Governing I-CAES

Several thermodynamic definitions are essential for a better understanding of the techniques used in the I-CAES technology to improve the system efficiency. An Isothermal process means a constant temperature (*Raible M., 2016: 16*).

$$T_1 = T_2 = \text{constant} \rightarrow \Delta T = 0$$

Figure 15 shows the pressure-volume diagram for the stages of a CAES system (i.e., the compression and expansion stages). The process starts by allowing the air to enter the compressor at atmospheric pressure and ambient temperature (Figure 15.a, point 1); the compressor compresses the air till it reaches the maximum pressure at point 3 and then sends the compressed air to the reservoir. The expansion process takes place from point 3 to point 1. The work done by the compressor is equal to the area between the x-axis and the compression curve, i.e., points 1,2,3. On the other hand, the expansion process is represented by the area between the vertical-axis and the expansion curve, i.e., points 3,4 (Figure 15.a). The difference between the expansion and the compression areas is significant for the reason that the work done by the compressor is much more than the work extracted from the expansion process which means, the efficiency of the system is relatively low due to the loss of energy. In Figure 15.b, a heat transfer enhancement has been made to save part of the work input for the compression process resulting in improving the efficiency of the system. Figure 15.c represents an isothermal process where the work input is very close to the work consumed by the expansion process giving the best efficiency we can get.

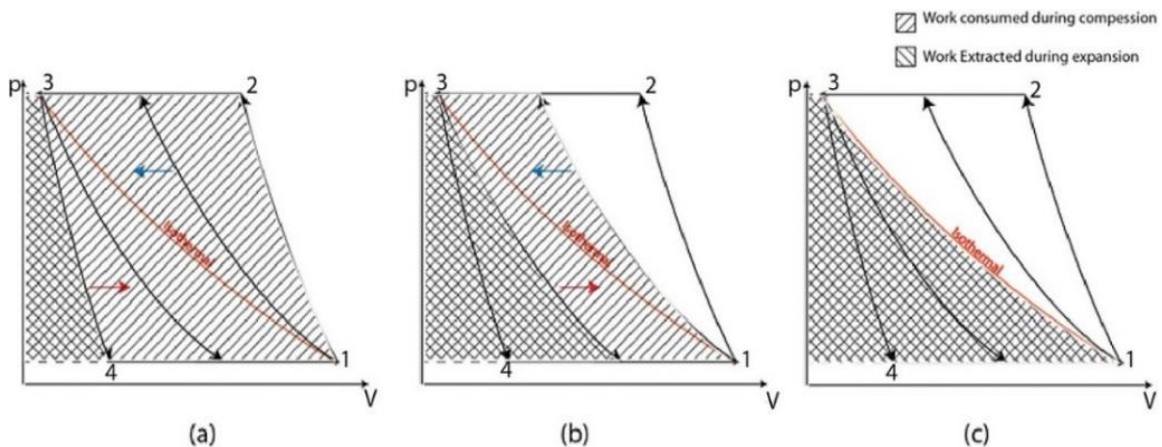


Figure 15: P-V diagram for CAES system (**Source: Heidari M. et al., 2017: 1253**)

The relationship between the pressure and the volume in a thermodynamic process is described in **Equation 3** (the polytropic equation) (*Al Shemmeri, T., 2010: 12*). The polytropic equation can describe the compression and the expansion processes which include heat transfer, work input and difference of input and output enthalpy (*Heidara M. et al., 2017: 1254*).

$$pV^n = C \quad (3)$$

Where:

- $p \rightarrow$ The pressure
- $V \rightarrow$ The volume
- $n \rightarrow$ The polytropic factor
- $C \rightarrow$ Is a constant

n is equal to 1.4 for an adiabatic process and 1 for an isothermal process (*Heidara M. et al., 2017: 1254*). We notice in **Figure 16** that as the polytropic factor decreases the heat transfer increases (*Heidara M. et al., 2017: 1254*).

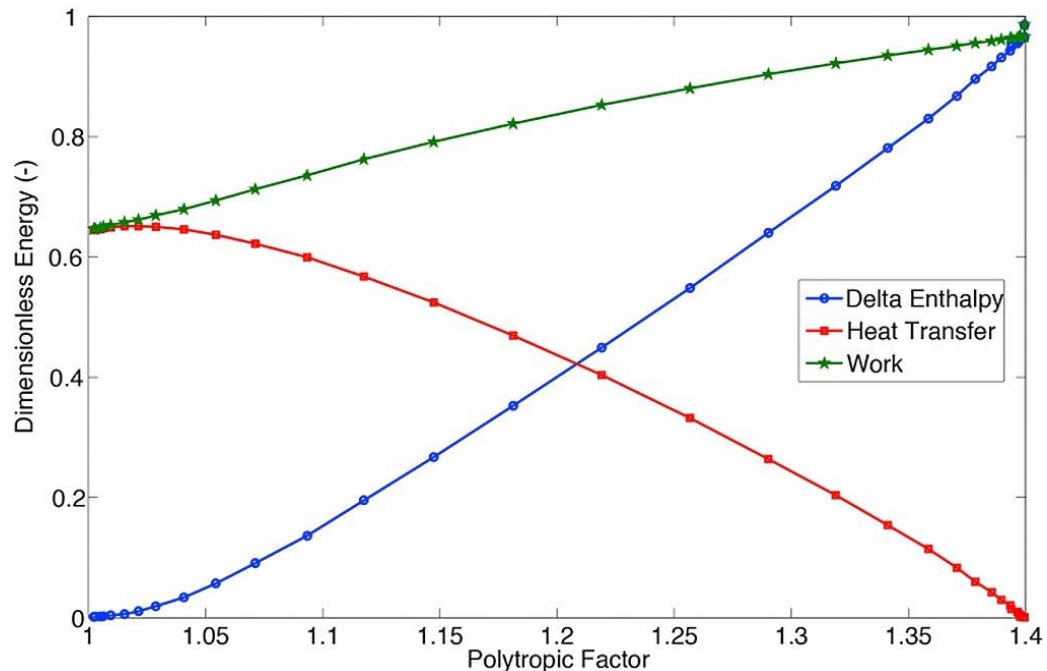


Figure 16: heat transfer rate and work change with the polytropic factor (**Source: Heidari M. et al., 2017: 1254**)

According to the first law of thermodynamics (**Equation 4**), the internal energy of a system (ΔU) increases with the increase of the amount of heat (Q_{in}) absorbed by the system (*Raible M., 2016: 14*).

$$\Delta U = Q_{in} - W_{out} \quad (4)$$

Where:

- $W_{out} \rightarrow$ The output work

Another important thermodynamic definition is the heat capacity (C). The heat capacity is determined by the amount of heat (ΔQ) needed to raise one Kilogram (kg) of a matter's temperature by one degree Celsius ($^{\circ}\text{C}$), and it is calculated using **Equation 5** (*Raible M., 2016: 15*). Each matter has a different heat capacity making some matters extremely useful for a particular usage.

$$C = \frac{\Delta Q}{\Delta T} \quad (5)$$

Specific heat has two values, C_p and C_v . C_v Is the change in internal energy (U) concerning the change of temperature with a fixed volume. C_p Is the change in enthalpy (H) concerning the change of temperature with fixed pressure, and the ratio of them (γ) is shown in **Equation 6** (*Raible M., 2016: 15*).

$$\gamma = \frac{C_p}{C_v} \quad (6)$$

In addition, giving the equation of the ideal gas (**Equation 7**), we know that the pressure of the gas multiplied by the volume of the gas ($P.V$) is constant in an isothermal process since the number of molecules (n), the universal gas constant (R), and the temperature (T) in Kelvin are constants (*Raible M., 2016: 16*).

$$P.V = n.R.T \quad (7)$$

$$R_{\text{air}} = 287.058 \text{ JK}^{-1}\text{kg}^{-1}$$

The average atmospheric pressure (p_o) at sea level is:

$$p_o = 101,325\text{Pa}$$

Though, the pressure (P) of a fixed mass of a gas is in reverse proportion to the volume (V) of the gas (**Equation 8**). This is known as Boyle-Mariotte's Law. The law says *“the volume of a given amount of gas held at a constant temperature varies inversely with the applied pressure”* (Fidalgo J. & Rañal F., 2014: 39). He also said that for this equation to be valid, the temperature of the gas has to be constant, in another word, Isothermal. That is why, in **Figure 17**, the curves varies for each temperature (Fidalgo J. & Rañal F., 2014: 39).

$$V \propto \frac{1}{P} \quad (8)$$

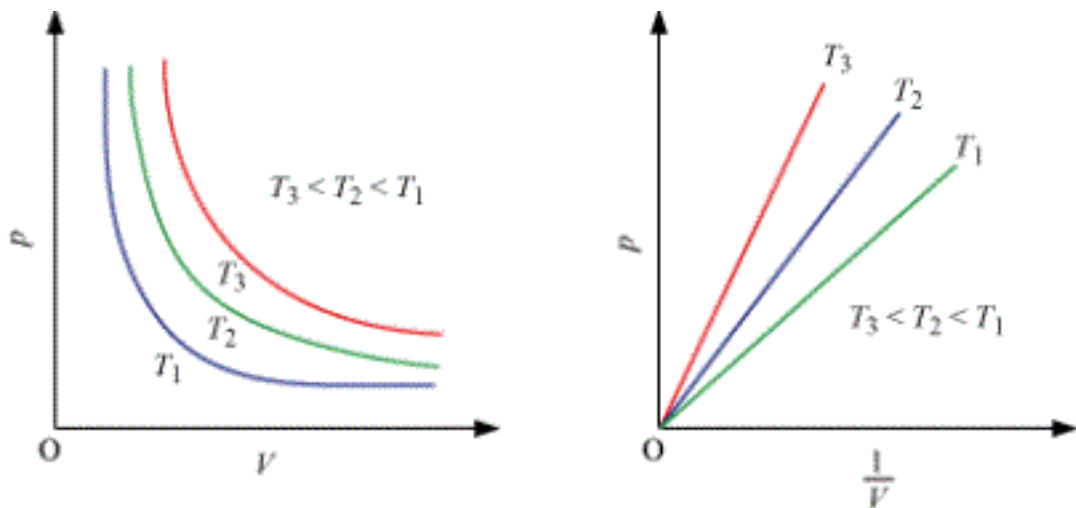


Figure 17: P-V diagram for the isothermal process (Source: Fidalgo J. & Rañal F., 2014: 39)

The pressure of the air entering the compressor is assumed to be the average atmospheric pressure, and in case of an installation of a CAES system above sea level by 500 m, the pressure is reduced to $p_o = 95,165 Pa$ (Gavery S. D. & Pimm A., 2016: 90). Once the air enters the compressor, the compressor compresses it to a higher pressure (p_1), and the pressure ratio (r) is defined by **Equation 9** (Gavery S. D. & Pimm A., 2016: 90).

$$r = \frac{p_1}{p_o} \quad (9)$$

Usually, for CAES systems, r is between 20 and 200 (Gavery S. D. & Pimm A., 2016: 90). As mentioned before, when the air is compressed, it generates heat. We can calculate the heat of the air after the compression process using **Equation 10** (Gavery S. D. & Pimm A., 2016: 90).

$$\frac{T_1}{T_o} = \left(\frac{p_1}{p_o}\right)^x \quad (10)$$

Where:

$$x = \left(\gamma - \frac{1}{\gamma}\right) \quad (11)$$

In an isothermal process, the work required to compress V_o of air from P_o to P_1 is calculated using **Equation 12** (Gavery S. D. & Pimm A., 2016: 92x).

$$W_{\text{isoth}} = P_o V_o \log(r) \quad (12)$$

To know exactly how much mass and volume of air the compressor can compress for an isothermal process, assuming $T_o = 300 K$, we need to know the pressure ratio (r) and the energy available to drive the compressor. The following table gives quantities of air that can be compressed by 1 Kwh for different pressure ratios (r).

Table 9: Quantities of air can be compressed with 1 kWh of work (Source: Gavery S. D. & Pimm A., 2016: 93)

Pressure ratio (r)	Isothermal Compression	
	Mass air /kg	Volume air /m ³
2	60.31	51.26
5	25.97	22.08
10	18.51	15.43
20	13.95	11.86
50	10.69	9.082
100	9.078	7.715

Using **Table 9** as a default is extremely useful in conducting assessments of intake flow rates of compressors giving the energy available for the process. If we take as an example an I-CAES plant with 50,000 *KWh* of energy available and r of 100, using the information given, we can calculate the air mass flow rate (\dot{m}_{air}) of the compressor simply by multiplying 50,000 *KWh* by the mass of the air (m_{air}) for the 1 *KWh* plant (9.078 *kg/h*) for $r = 100$.

$$\begin{aligned}
 \dot{m}_{air} &= E \times m_{air} \\
 &= 50,000 \text{ KWh} \times 9.078 \frac{\text{kg}}{\text{h}} \times \frac{1 \text{ h}}{3600 \text{ s}} = 126.1 \frac{\text{Kg}}{\text{s}}
 \end{aligned}
 \tag{13}$$

2.6. Current Development of the I-CAES technology

➤ LightSail Energy company

The Company was founded in 2008 by Danielle Fong and is based in Berkeley, California (*Taranovich S., 2012*). LightSail's idea of implementing an I-CAES system is to capture the heat by injecting a fine, water spray creating a mist dense to absorb the heat and store it for later use during the expansion process (*Taranovich S., 2012*). Danielle Fong chose to use water for the reason that water has a high heat capacity which means it can absorb a large amount of heat per *Kg* injected (*Taranovich S., 2012*). Another key factor in the idea is, to have a large spraying area to speed up the rate of heat transfer and maintaining a near the isothermal process.

First, during the compression process, the mechanical energy is converted to heat; then a fine, dense water spray is injected directly into the compressed air to absorb the heat. The use of water is due to the high heat capacity it has which is 3,200 times the heat capacity of air. The compressed air is stored in low-cost tanks that meet safety standards, and the warm water passes through the heat exchanger. Finally, during the expansion process, the water passes again through the heat exchanger, and the heat is then added to the compressed air and converted into mechanical work to generate energy (*Taranovich S., 2012*).

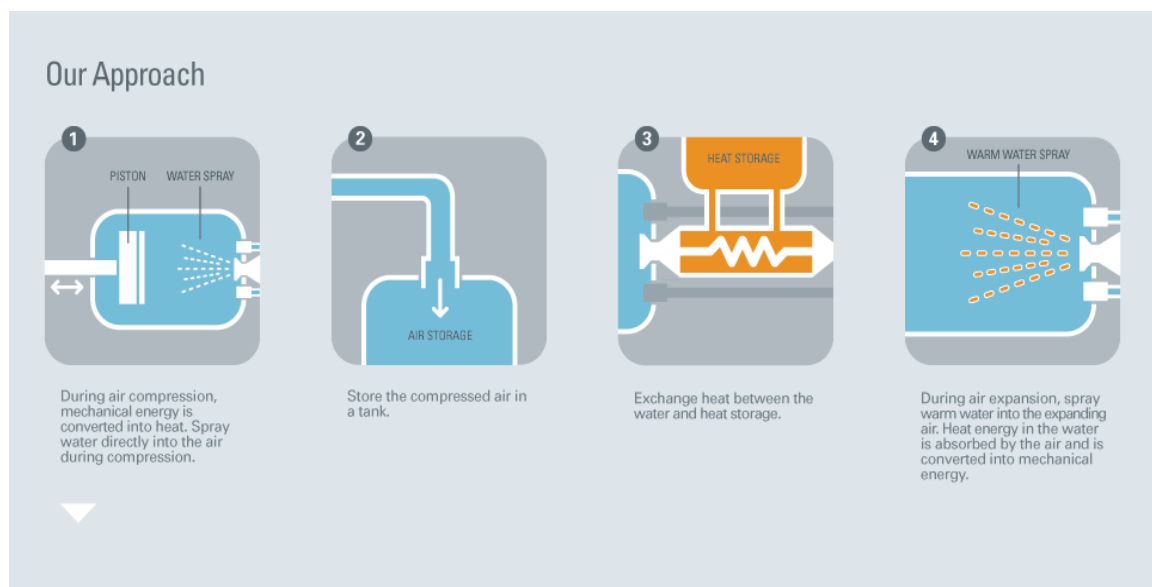


Figure 18: I-CAES LightSail Company's Approach (*Taranovich S., 2012*)

The company LightSail Energy publicly announced its targets for the I-CAES system to achieve. These targets are as follows (EPRI, 2015: 2):

- Capital cost of 500 \$/kW and 100 \$/kWh
- Round-trip efficiency of 70% (no added heat)
- Power density of 200 W/kg
- Energy density of 33.3 kWh/m³
- Efficient utilization of waste heat

To achieve these targets, LightSail Energy uses special equipment and methods, for instance, a modified reciprocating compressor, i.e. an Ariel JGJ/4 gas compressor (**Figure 19**); The company also uses multiple compression stages to achieve the final desired pressure (EPRI, 2015: 2).

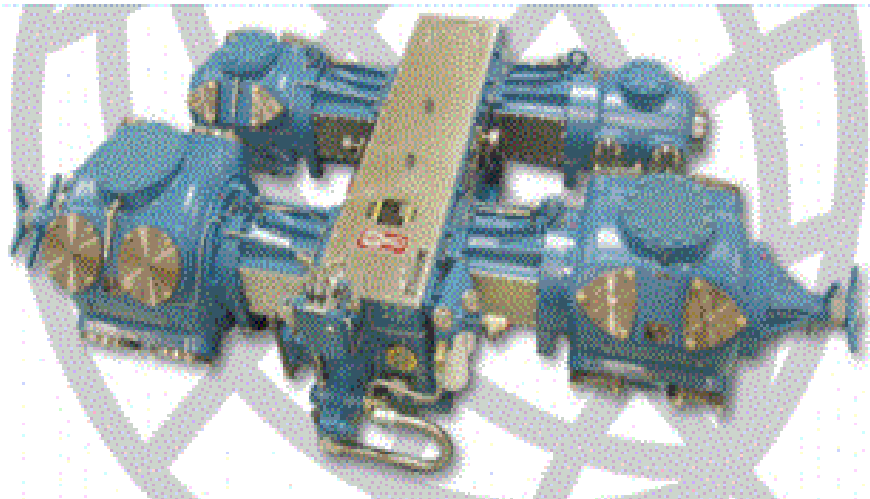


Figure 19: a LightSail modified reciprocating compressor (Source: EPRI, 2015: 2)

Moreover, the technology is developed to be a reversible process, which means, during the compression process, an electric motor runs the compressor, and during the expansion process, the same compressor becomes an expander, and the same electric motor becomes a generator leading to a dramatic reduction in cost dramatically (Taranovich S., 2012).

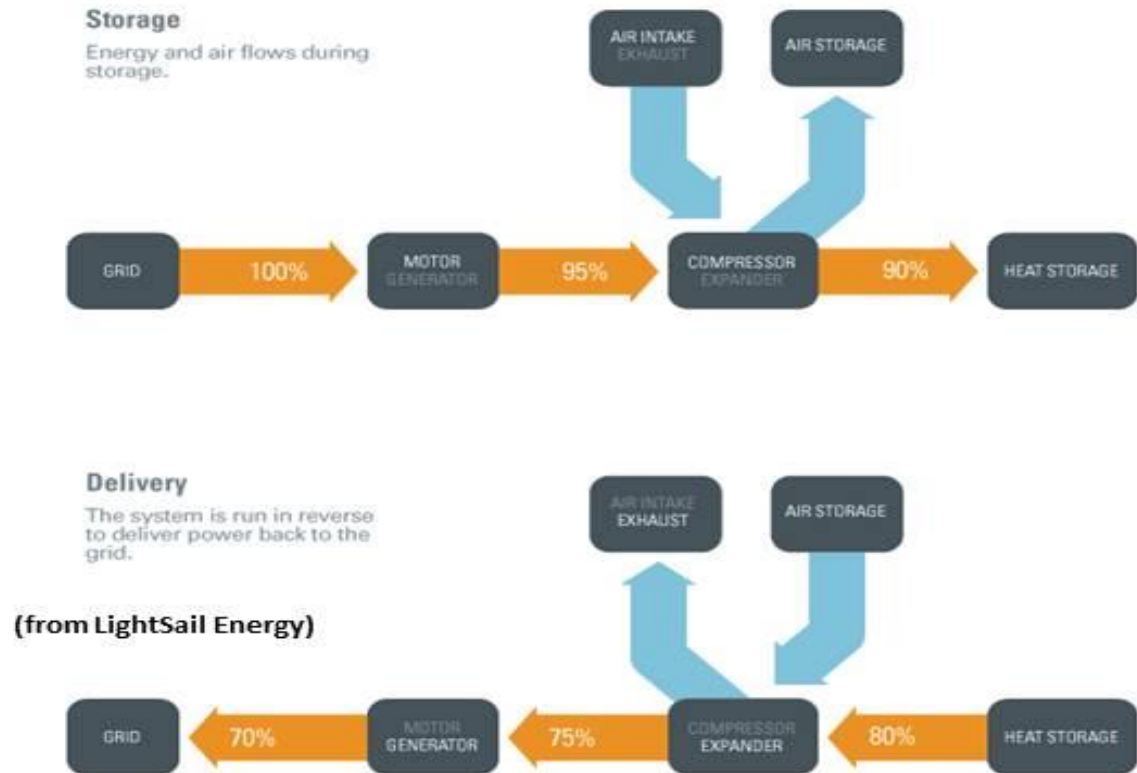


Figure 20: Illustration of the reversible process of I-CAES system from LightSail Company
(Source: Taranovich S., 2012)

The experimental result exposed by the company shows that achieving higher thermodynamic efficiency is possible without a reduction in performance. The key is, achieving the highest possible RPM, for the reason that, the higher the RPM, the higher is the output power and the lower the cost per *kW* (Taranovich S., 2012). **Table 10** presents the experimental efficiency result.

Table 10: LightSail's Experimental Efficiency Result for the I-CAES system (Source: Taranovich S., 2012)

Thermal Efficiency (%)	Final Temperature Difference (°C)	RPM	Maximum Power achieved (KW)	Operational hours
90	< 10	1200	100	500+

When producing a small amount of energy, underground storage is not economically feasible, that is why the LightSail Energy company came up with low-cost storage tanks made out of industrial standard pipes (meeting ASME and ISO safety standards), put inside a shipping container (**Figure 21**).



Figure 21: Low-cost storage containers within a shipping container (Source: Taranovich S., 2012).

➤ **SustainX company**

SustainX is another company marketing the I-CAES technology. They are also using a technique to store the heat generated from the mechanical work and then reuse it to heat the compressed air during the expansion process. The technique the company uses is to keep the air in direct contact with the water during the compression process to ensure a good heat transfer from the compressed air to the water. The company was founded in 2007. Since then it went through a development in three major stages (*EPRI, 2015: 1*): **(i)** In 2009, a 1 KW I-CAES system was built to demonstrate the effectiveness of the technology, **(ii)** In 2010, an I-CAES pilot project was implemented with a capacity of 40,

the pilot project proves the effectiveness of the technology and gave lessons to develop a commercial-scale system based on an isothermal process (*SustainX, 2015: 6*), and (iii) The last stage was a commercial-scale system with a capacity of 1.5 MW, this project is now operating since 2014 (*SustainX, 2015: 34*).

The 1.5 MW prototype consists of six cylinders to provide two compression stages, three low pressure (from 0 to 180 psig) and three high pressure (from 180 to 3,000 psig) connected to a crankshaft that moves the piston through a reciprocating motion (**Figure 22**) (*SustainX, 2015: 16*). To achieve cost-effectiveness and improved efficiency; SustainX uses marine diesel reciprocating engine that offers high compressions ratio. **Figure 22** shows the marine diesel reciprocating engine in the compression and expansion process; it also shows how the overground storage system looks like. As indicated in **Figure 22**, the 1.5 MW system reaches full power in 60 seconds; switch from charging to discharging mode in 5 seconds; takes 8 hours to fully charge and 6 hours to discharging (*EPRI, 2015: 2*).

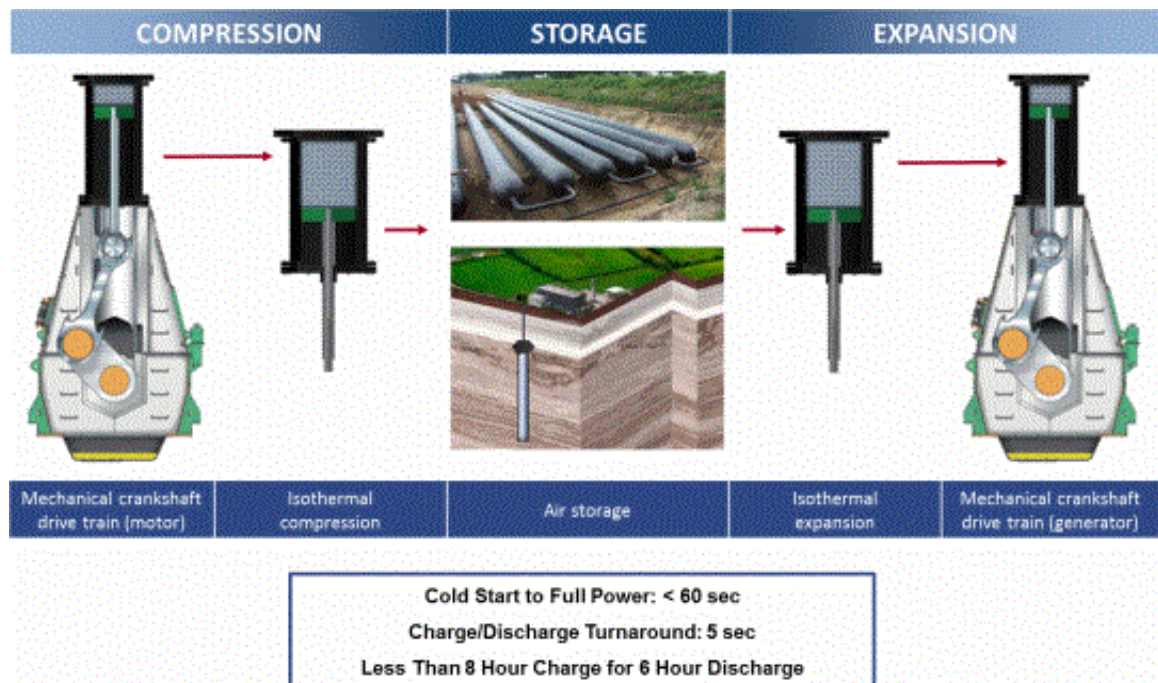


Figure 22: SustainX compression/expansion of the marine diesel reciprocating engine and an illustration for the storage reservoir (*EPRI, 2014: 5*)

3. Method of Approach

This thesis applies a documentary analysis approach to obtain data. First, background information on ESS technologies in general and the CAES technology in specific was presented in chapter 2 using a literature study. The background information discussed the characteristics of ESS technologies and the applications in which the ESS could support, in addition, the importance of the use of ESS technologies to achieve a sustainable energy system by improving the security of the energy supply, ensuring the safety of the grid, and improving the efficiency of RE systems. It also discussed the different CAES technology operational methods and the state-of-the-art of the technology to get an overview of the technology. Finally, the thermodynamics of the I-CAES technology was discussed along with the current development status to understand the science behind the technology and the status quo of the I-CAES technology.

To address the questions above in chapter 1 (section 1.2), the following tasks were carried out:

➤ Technological appraisal

Based on literature studies, researches, experimental results, and a case study, the technological part of the I-CAES technology was discussed as follow:

- To support RE systems effectively, a high-efficient ESS for bulk electricity applications is required. In order to calculate the efficiency, analyzing the energy/exergy cycle (from input to output) for an I-CAES system is crucial. The variable parameters for an I-CAES system are obtained from a study conducted by the Technical University of Denmark (*Brian E. & Brix W. M., 2011*), and the calculation of the efficiency is carried out using equations from the same study.
- Study the technology used to transfer heat to obtain a near-isothermal process, (i.e., Heat Transfer Based on Water Spray) by one of the leading companies in the I-CAES technology (SustainX). Experimental results from a computer modeling are used to determine the characteristics required to achieve an efficient heat transfer.

- Examine the potential of the I-CAES system to support off-grid applications. The biggest disadvantage of using the traditional CAES system, (i.e., D-CAES system) is the low efficiency the system has. For this reason, the D-CAES system is not able to support small-scale applications, (e.g., off-grid applications). In this paper, the potential of the I-CAES system is examined to support off-grid applications using experimental results from study conducted by the University of Arizona where they studied the performance of a small-scale off-grid PV systems integrated with a 160 W I-CAES system and they came up with the design specifications (*Villela, D., 2010*).
- A case study is presented to examine the potential of the I-CAES system to support wind power plants. A quantitative model-based approach is used in this part to perform some calculation in regard to the compressor size needed for the system. Also, a simulation for the actual and forecasted power generated by the wind farm is obtained from the study to discuss the performance of the system with and without a traditional CAES system and compare it to an I-CAES system.

➤ **Economic evaluation**

Based on case studies from different research institutions, the economical part of the I-CAES technology was discussed as follow:

- Description of the methodology used to facilitate the comparison between technologies, (i.e., the Levelized Cost of Electricity (LCOE)). In addition, present a sensitivity study conducted by the Department of Electrical & Computer Engineering, Portland State University, USA (*Obi M. et al., 2016*). The goal of this study is to determine the most sensitive parameters affecting the LCOE of the CAES system.
- Present a cost breakdown of the CAES system and describe how to calculate the cost of the system (power and energy-related costs).
- Present two case studies for traditional CAES, (i.e., D-CAES system) and examine the economic potential when substituting the D-CAES system with an I-CAES

system. The aim of this part is to see how the I-CAES system can affect the economic situation of the technology.

- CAES/Wind farm → a study conducted by the Iowa University to assess the economic feasibility for a D-CAES system when integrated with a 150 *MW* wind farm to store energy on a monthly basis. Then, examine the effect of the hybrid system when changing the storage system from D-CAES to I-CAES system.
- CAES/PV/Grid → a study from the Arizona Research Institute for Solar Energy (AzRISE) to examine the economic impact of three different scenarios for electricity generation, (i.e., (1) Grid+PV, (2) Grid+CAES, and (3) Grid+CAES+PV). Then, examine the effect of the hybrid system when changing the storage system from D-CAES to I-CAES system.
- Describe the economic differences between large and small-scale traditional CAES systems and compare it to the I-CAES system.

4. Technological Description

4.1. Efficiency of I-CAES

Any ESS requires a technical analysis to evaluate the technology before commercializing it. To know the efficiency of any system, we have to calculate all losses through the whole cycle (input to output). We can describe the efficiency of a storage system (η_{sc}) using **Equation 14** (*Brian E. & Brix W. M., 2011: 3*). We calculate the efficiency at the charging, storage, and discharging process then we apply the formula to get the overall system efficiency.

$$\eta_{sc} = \eta_{char} \times \eta_{stor} \times \eta_{disc} \quad (14)$$

Where:

- η_{char} → The charging efficiency
- η_{stor} → The storage efficiency
- η_{disc} → The discharging efficiency

When an ideal gas is compressed and then cooled down to return to its original temperature (ambient temperature), the heat loss is equivalent to the net-work done on the air to compress it. A perfect reversible process in the context of thermodynamics considers an ideal process because only then we can reach 100% efficiency. For instances, when we mix two fluids with a finite temperature difference, it becomes an irreversible process which means that we lose almost all the energy invested in the first place. The term “exergy” indicates the amount of work extracted from a system until it reaches an equilibrium with the environment (*Garvey S. D. & Pimm A., 2016: 109*). It is important to know that when storing an amount of heat (ΔQ) under T_1 , the exergy (ΔE) is calculated using **Equation 15** (*Garvey S. D. & Pimm A., 2016: 95*). By calculating the exergetic efficiency of all steps of the storage process, we can determine the overall system efficiency and distinguish between losses due to charging, storing and discharging (**Equation 16,17,18,19**) (*Brian E. & Brix W. M., 2011: 5-6*).

$$\Delta E = \Delta Q \times \left(1 - \frac{T_0}{T_1}\right) \quad (15)$$

$$\eta_{sc} = \eta_{char} \times \eta_{stor} \times \eta_{disc} = \eta_{x,c} \times \eta_{x,stor} \times \eta_{x,t} \quad (16)$$

Where:

- $\eta_{x,c} \rightarrow$ The exergy efficiency of the compressor
- $\eta_{x,stor} \rightarrow$ The exergy efficiency of the storage reservoir
- $\eta_{x,t} \rightarrow$ The exergy efficiency of the turbine

The exergy efficiency of the compressor, the storage reservoir, and the turbine can be calculated using the following equations:

$$\text{Compressor} \rightarrow \eta_{x,c} = \frac{\Delta E_1}{W_c} \quad (17)$$

$$\text{Storage} \rightarrow \eta_{x,stor} = \frac{E_3}{E_2} \quad (18)$$

$$\text{Turbine} \rightarrow \eta_{x,t} = \frac{W_t}{\Delta E_{34} + E_f} = \frac{W_t}{E_3} \quad (19)$$

Where:

- $E_1 \rightarrow$ The exergy to the compressor inlet
- $E_2 \rightarrow$ The exergy to the storage inlet
- $E_3 \rightarrow$ The exergy from the storage outlet
- $E_4 \rightarrow$ The exergy from the turbine outlet
- $E_f \rightarrow$ The exergy of the inlet fuel
- $W_t \rightarrow$ The work done to the turbine
- $W_c \rightarrow$ The work done by the compressor

In the case of an isothermal process, the energy/exergy flow is a little bit different. To better understand the process, assume an I-CAES system with an output of 1 kWh (Figure 23).

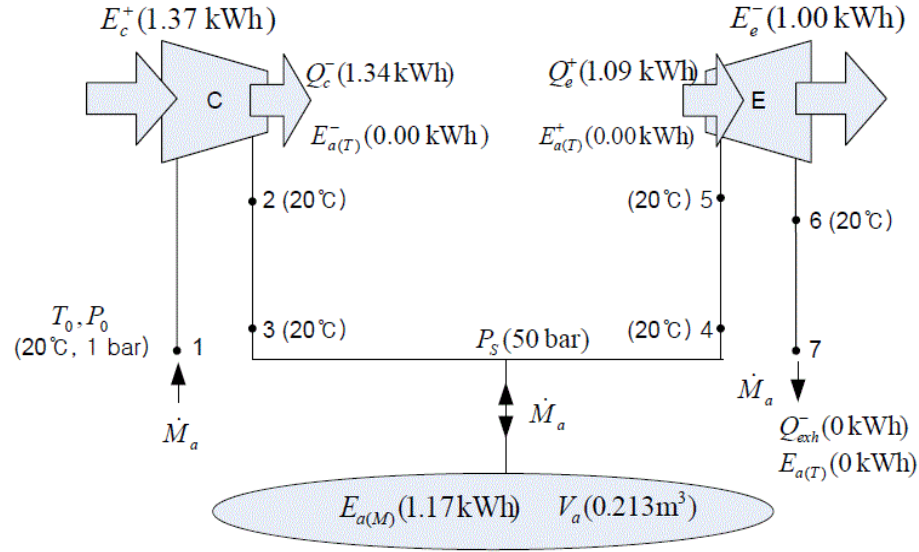


Figure 23: Energy/Exergy flow of the I-CAES system (Source: Kim M. Y., 2012: 22)

The air is compressed isothermally up to 50 bar and then stored; after that, the compressed air is expanded isothermally. In order to calculate the work done throughout the compression and expansion process, Equations 20 & 21 are used (Kim M. Y., 2012, p: 21).

$$W_{c,t}^+ = M_a \times (q_{c,t}^- + \Delta h) = M_a \times (-T_c \Delta s + \Delta h) \quad (20)$$

Where:

- $W_{c,t}^+ \rightarrow$ The compression work for an isothermal process
- $M_a \rightarrow$ The air mass entering the compressor
- $q_{c,t}^- \rightarrow$ The output heat from the compressor for an isothermal process
- $\Delta h \rightarrow$ The difference in the enthalpy
- $T_c \rightarrow$ The temperature of the compressed air after the compression process
- $\Delta s \rightarrow$ The difference in the entropy

Or

$$W_{c,t}^+ = P_{atm} V_{exp} \left(\ln|r| + \frac{1}{r} - 1 \right) \quad (21)$$

Where:

- P_{atm} → The atmospheric pressure
- V_{exp} → The volume of the air after the expansion process
- r → The ratio between the atmospheric pressure and the air pressure after the compression process

And

$$W_{e,t}^+ = M_a \times (q_{e,t}^- - \Delta h) = M_a \times (T_e \Delta s - \Delta h) \quad (22)$$

Where:

- $W_{e,t}^+$ → The expansion work for an isothermal process
- $q_{e,t}^-$ → The output heat from the expansion process for an isothermal process
- T_e → The temperature of the air during the expansion process

The isothermal efficiency of the compression and expansion process $\eta_{c,t}$ & $\eta_{e,t}$ respectively, can be calculated using the following equations (Kim M. Y., 2012, p: 21).

$$\eta_{c,t} = \frac{W_{c,t}^+}{W_c^+} \quad (23)$$

$$\eta_{e,t} = \frac{W_{e,t}^-}{W_e^-} \quad (24)$$

Where:

- W_c^+ → The actual work done by the compressor
- W_e^- → The actual output work from the expansion process

4.2. Heat Transfer Based on Water Spray for I-CAES

An effective heat transfer between the compressed air and the water is key factor for a high-efficiency I-CAES system. The heat transfer through spraying water happens in both compression and expansion phases in which five points need to be taken into consideration (*SustainX, 2015: 19*).

- [1] The distance between the water and the air has to be the minimal.
- [2] The water spray has to cover the whole area where the compression and the expansion processes take place.
- [3] A uniform distribution of water droplets.
- [4] Maximum contact surface area between the water's nozzles and the area in which the compression and the expansion processes take place.
- [5] Minimum energy usage for the generation of water droplets.

Spraying water at atmospheric pressure is well know, but when it comes to spraying water at high-pressure conditions, experiments need to be done in order to come up with the droplet sizes and distributions that achieve the highest thermal efficiency possible. SustainX company built a high-pressure, liquid-in-air machine (HPLIA) to test and see the characteristics of water droplets when spraying at different pressure levels, different nozzles and different operating conditions (**Figure 24**) (*SustainX, 2015: 19*).

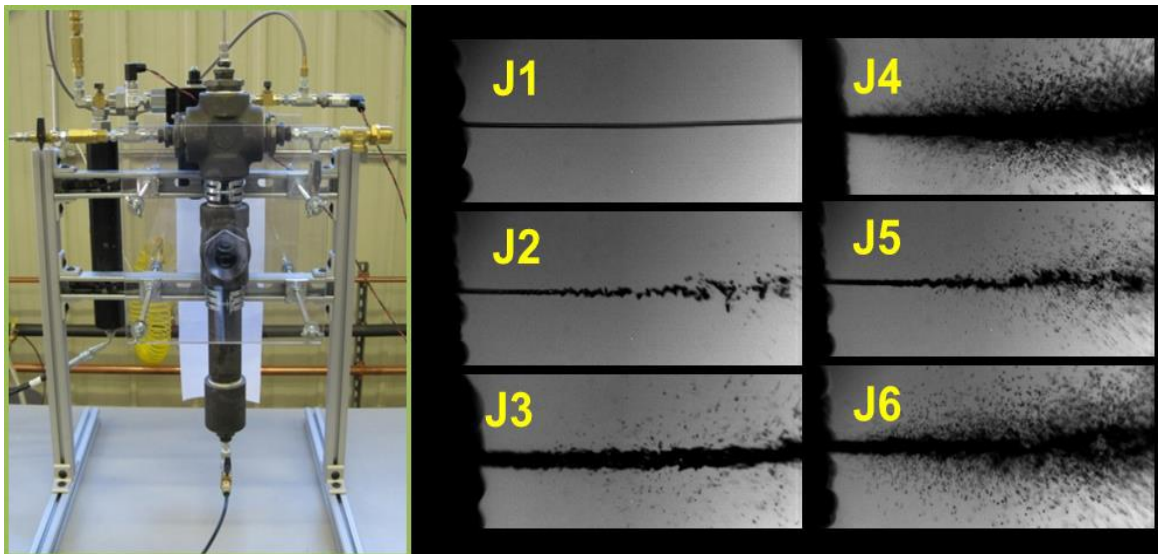


Figure 24: HPLIA Machine for testing spraying water under different conditions (**Source:** *SustainX, 2015: 19*)

A HPLIA machine uses computer modeling to come up with the characteristics required to achieve the best heat transfer efficiency given all the information needed, i.e., injection velocity, air density, stroke/dwell times and other constraints (*SustainX, 2015: 19*). The experiment was done under the following conditions:

- Air pressure: 1 – 69 bar (15 – 1000 psia)
- The differential injection pressure: 0.35 – 3.45 bar (5 – 50 psid)

The test results for different air pressures and differential injection pressures show that water droplets of $100\ \mu\text{m}$ – $900\ \mu\text{m}$ are required for optimal heat transfer between the compressed air and the water (*SustainX, 2015: 19*). The test also show that for a injection at 2 bar differential pressure and an air pressure above 60, the spray nozzles J6 is the result and, for air pressure above 20 bar, the results are J4 and J5 (*SustainX, 2015: 19*). The goal of this experiment is to choose the potential nozzles that could achieve the desired results and then do further experimentation.

SustainX also conducted another experiment to test the effectiveness of water in absorbing heat (The isothermal efficiency). They built another machine called Heat Transfer Test Stand (HXTST) (**Figure 25**) (*SustainX, 2015: 20*). This machine demonstrates the whole cycle of an I-CAES (Compression & Expansion process).

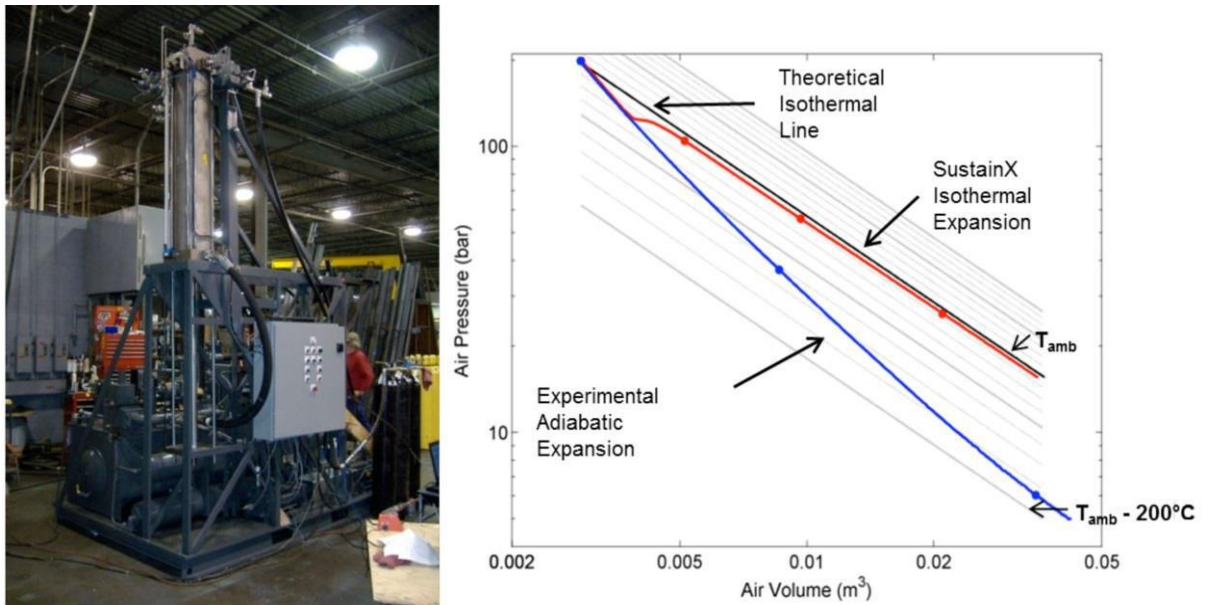


Figure 25: Heat-transfer test stand (HXTST) and Experimental results (**Source: SustainX, 2015: 20**)

First, the air goes into the compressor chamber at a pressure of 17.2 bar; then the hydraulic fluid pushes the piston upwards to compress the air to 207 bar (work done between 25 *kW* and 75 *kW*). During the compression stroke, the water spray is injected (up to 7.6 liter). When the expansion process starts, the piston goes down as the air enters the chamber and the process is repeated (*SustainX, 2015: 20*).

Figure 25 shows the results done on two expansion processes, an Adiabatic expansion, and an Isothermal expansion. During the adiabatic expansion, no water spray was added, and the process took 2.3 seconds; as we can see in the figure, the temperature decreases 175 °C from the starting ambient temperature. The efficiency of the adiabatic expansion is 54%. For the second expansion phase (the isothermal expansion), water spray was added after 0.5 seconds from the starting point. The compressed air maintained 15 °C difference from the ambient temperature (the difference between the black and the red line). The isothermal process achieved 95% thermal efficiency, and it took 3.8 seconds, that's 65% longer than the adiabatic process. The reason for that is, the heat from the water helps to maintain a higher air pressure throughout the whole expansion process (*SustainX, 2015: 21*).

4.3. I-CAES / Off-Grid System

One of the biggest disadvantages of traditional CAES systems is that they are not economically feasible for small-scale applications because of its low efficiency. Many of the rural areas around the world especially in Africa have no access to energy for daily use, e.g., lighting and cooking. RE stand-alone (off-grid) systems came as an affordable solution particularly PV technologies (**Figure 26**). There are around 133 million people in Africa that have access to light (< 11 watts) and electricity at home (> 11 watts) through solar technologies (*IRENA, 2018: 4*). To make these RE technologies reliable and make it accessible whenever it's needed, we need small-scale storage systems, and it has to be economically feasible when integrated with RE systems.

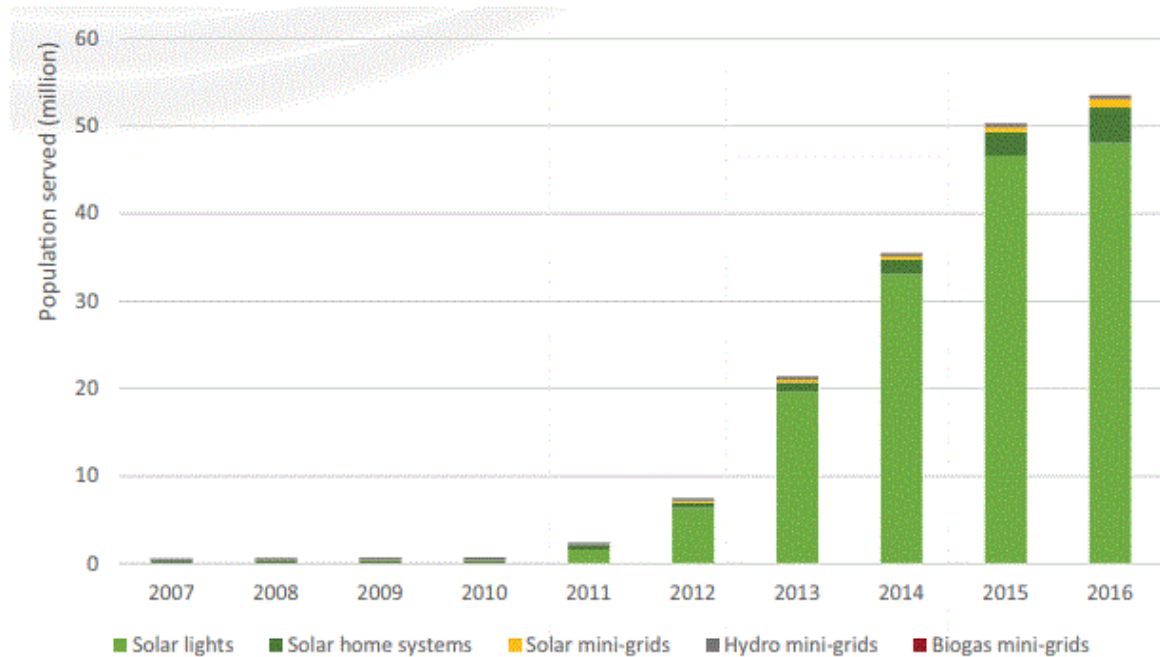


Figure 26: Population served by off-grid RS technologies in Africa (**Source: IRENA, 2018: 4**)

I-CAES could be a potential solution for off-grid RE applications. An I-CAES system has a high overall system efficiency that makes it reasonable to use it in small-scale systems. However, only a high efficiency is not enough to make the hybrid system feasible. We also need to reduce the cost of building the system, and the way to do that is to get rid of some unneeded parts for small-scale systems, i.e., we can sacrifice a small amount of the system's efficiency in return of some of its parts. For example, develop a single stage compression/expansion system instead of a multiple stage system, in addition, the use of low cost, a small-scale piston-driven compressor that operates at compression rates between 10 – 60 rpm (*Villela D. et al., 2010*). Usually, large-scale CAES systems use multiple compression/expansion system to reach high compression rates and produce more energy, but in our case, we do not need a large amount of energy, for the system to be economically feasible we need to reduce the cost of the system and produce a small amount of energy. Another important thing is the type of compressor used in the system. Liquid-piston based compressors (**Figure 27**) are always recommended in small-scale systems because they increase the volumetric efficiency and reduce dead volume (*Villela D. et al., 2010: 3*).

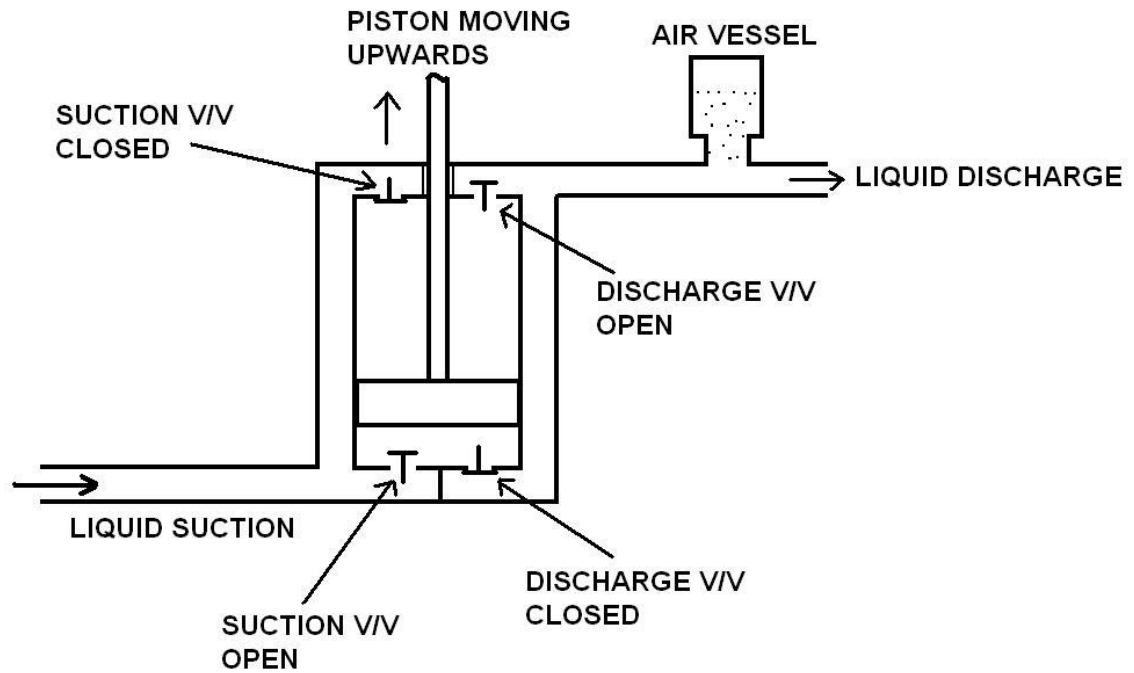


Figure 27: A simplified illustration of the liquid piston (Taylor D. A., 1996: 115)

The University of Arizona has proposed small-scale off-grid PV systems integrated with a 160 W I-CAES system (Villela D. et al., 2010: 3). The proposed compressor prototype has the following criteria (Villela D. et al., 2010: 4):

- [1] Liquid-piston based compressor.
- [2] Stainless steel cylinder with a high aspect ratio for increased thermal conduction.
- [3] The timed electronic valve in synchronization with the stroke speed for optimal flow of compressed air into the storage tank.
- [4] Low-friction moving parts to minimize energy losses.
- [5] Mechanically robust to shear cracks.

The design is made in a way that the piston dimensions and the stroke length match the pressure ratio that achieves the best efficiency. In an isothermal process where the mass of the air is fixed, we can calculate the final pressure using **Equation 10**. The maximum stroke speed reached by the prototype is 63 rpm under $\pm 2^{\circ}\text{C}$ the difference in temperature which comes close to an isothermal process because the temperature difference is almost negligible (Villela D. et al., 2010: 5).

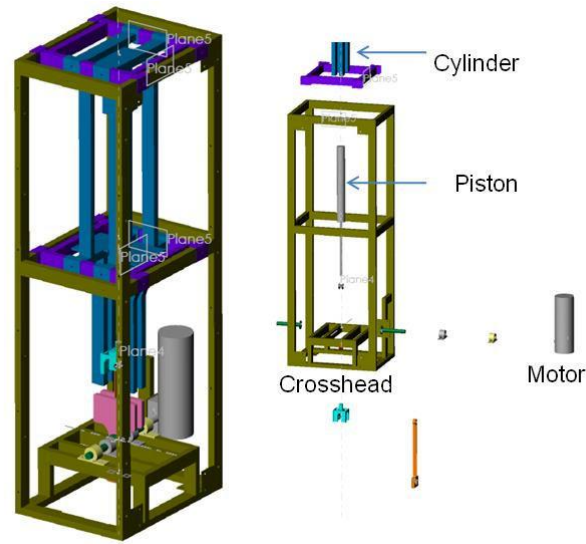


Figure 28: The compressor developed prototype (Source: Villela D. et al., 2010: 4)

Figure 29 illustrates the efficiency of the system as a function of the compression rate (rpm). From the figure, we can see that, when operating at the maximum compression rate, the efficiency of the system is as low as 40%, and the maximum efficiency (70%) can be reached when operating at 15 rpm at an operating power of up to 25 watts (Villela D. et al., 2010: 5). Further research is ongoing in order to study the possibility of developing a system that can deliver more compression work (rpm) with higher efficiency (Villela D. et al., 2010: 6).

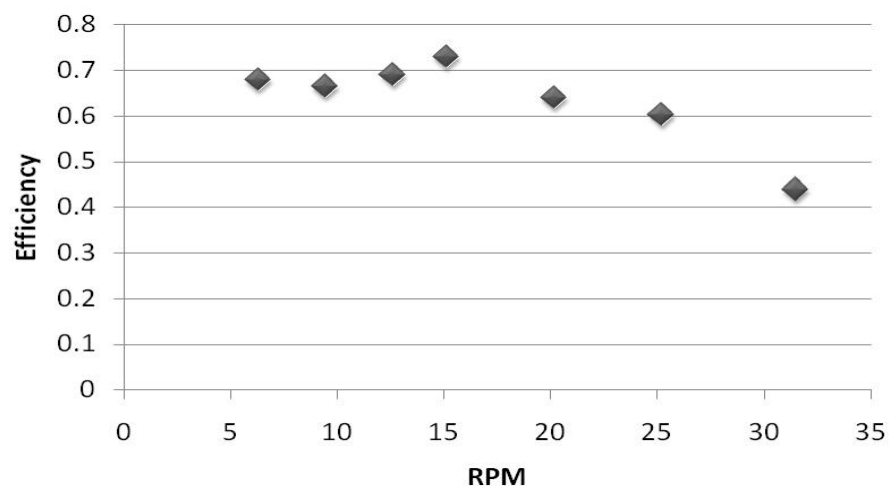


Figure 29: The system efficiency as a function of the compression rate (rpm) (Source: Villela D. et al., 2010: 5)

4.4. I-CAES / Wind Power

ESS have a great benefit when integrated with RE systems especially when combined with the technologies that have intermittent resources such as solar and wind. Many countries are trying to increase their electricity production from RE sources for the many benefits mentioned before. That is why, expanding the installation of wind power plants in particular is the target for many governments around the world, due to the high potential of energy production the technology has, e.g., the U.S Scenario: 20% of the country's electricity production should come from wind power by 2030 (*U.S. Department of Energy, 2008: 1*).

Integrating an I-CAES system with off-shore wind turbines can also increase the efficiency dramatically because it can eliminate the need to generate electricity two times. When the blades of the turbine move due to the movement of wind, the blades of a turbine move at a rate that is too slow to produce electricity directly, that is why a gearbox is used (*Li P. Y. et al., 2015: 3*).

The CAES system removes the need for a gearbox and the associated losses leading to a reduction in cost and an increase in the efficiency (*Li P. Y. et al., 2015: 7*). In an I-CAES/Wind turbine hybrid system (**Figure 30**), instead of a gearbox, the shaft is connected to a hydraulic pump. The power generated by the hydraulic pump operates the hydraulic transformer providing the movement of the liquid piston to perform the compression and expansion processes. On the other hand, valves that exist on the top of the liquid piston chamber (**Figure 31**) control the air flow, during the compression phase when the atmospheric pressure is larger than the pressure inside the chamber, the valves open up, and the air is drawn into the chamber. The liquid piston moves and compresses the air until another valve that is connected to an open accumulator is opened, and the compressed air goes into it (*Li P. Y. et al., 2015: 4*).

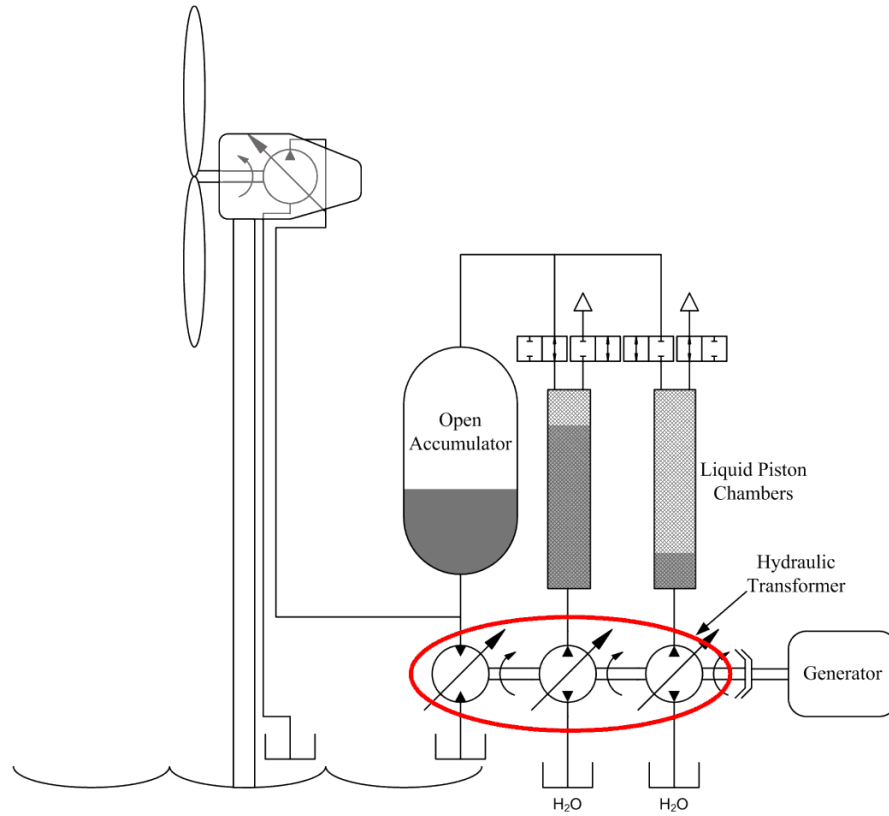


Figure 30: CAES/Wind turbine hybrid system (Source: Li P. Y. et al., 2015: 4)

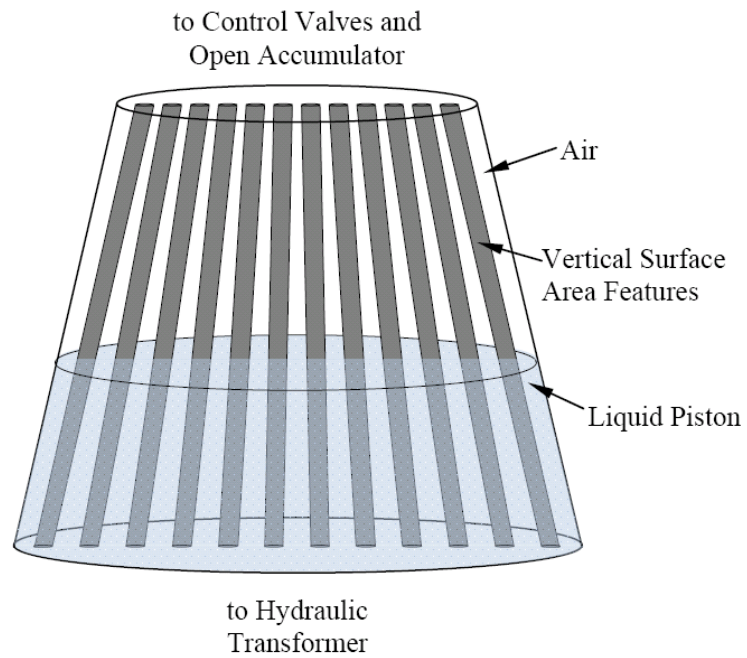


Figure 31: The liquid piston chamber (Source: Li P. Y. et al., 2015: 4)

To get a better understanding of how an I-CAES system and a wind turbine are combined and function as one system. Assuming an off-shore wind turbine, that operates and generates a maximum power of 5 MW. Because the wind blows in non stable manner, a 3 MW power for 8 hours a day is assumed. The first step to design a storage system is to calculate the energy produced. All the values that will be assumed in this example are taken from a report produced by a joint research done by the University of Minnesota, the University of Virginia, Worcester Polytechnic Institute, and LightSail Energy, Inc (Li P. Y. et al., 2015: 4).

$$E = P \times T = 3 \text{ MW} \times 8 \text{ hours} = 24 \text{ MWh} \quad (25)$$

$$24 \text{ MWh} = 24 \text{ MWh} \times 3600 \frac{\text{seconds}}{\text{hour}} = 86,000 \text{ MJ} \cong 86 \text{ GJ} \quad (26)$$

Assuming:

- Liquid Piston Compressor
- A compression pressure of 1 MPa
- Air volume entering for each cycle = 6.12 m³
- $V_{\text{exp}} = 176,350 \text{ m}^3$
- Spherical open accumulator with an inner radius of 4.95 m
- Heat transfer rate (H_R) = $100 \frac{\text{W}}{\text{K}} / \text{m}^2$
- The temperature difference between the chamber and the compressed air $\Delta T = 5 \text{ K}$
- Area of the heat transfer surface = 12,000 m²

Knowing that:

- 1 atm = 101,35 KPa = 0.101035 MPa

Using **Equation 9** to calculate the pressure ratio (r):

$$r = \frac{35}{0.10135} = 347 \quad (27)$$

$$V_{comp} = \frac{V_{exp}}{r}$$

$$= \frac{176,350 \text{ m}^3}{347} = 509 \text{ m}^3$$
(28)

The surface area to volume ratio:

$$\frac{\text{Heat transfer surface area}}{\text{the volume of atm air each cycle}}$$

$$= \frac{12,000 \text{ m}^2}{6.12 \text{ m}^3} = 1960 \text{ m}^{-1}$$
(29)

The liquid piston shown in Figure 32 consists of small diameter rods placed vertically in the chamber. The purpose of the rods is to act as temporary heat storage during the compression process. When the liquid piston returns to the starting point, the liquid absorbs the heat from the rods. The rods also increase the surface area to volume ratio (Li P. Y. et al., 2015: 4). There are different possible geometries for a liquid piston; **Figure 33** illustrates the geometry assumed in this example. The rods are placed vertically inside the chamber of the liquid piston. To facilitate the calculation of the surface area to volume ratio, the geometry of the chamber is divided into equilateral triangles as shown in **Figure 32**. It is important to note that the intersection of the triangle with the circles covers $\frac{1}{6}$ of each of the circles.

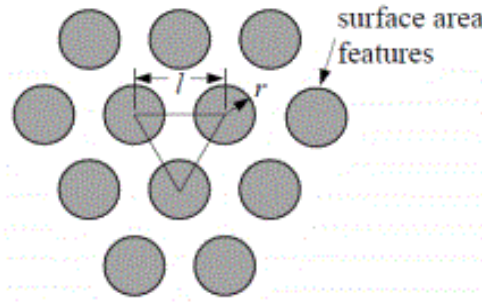


Figure 32: Rods inside the liquid piston chamber (Source: Li P. Y. et al., 2015: 6)

After dividing the shape, the first step is to calculate how much liquid volume there is within the triangle using the following formula (Li P. Y. et al., 2015: 6).

$$V = V_{triangle} - V_{rods} = \frac{\sqrt{3}}{4} l^2 - \frac{1}{2} \pi r^2 \quad (30)$$

Where:

- $V_{triangle}$ → The volume of the triangle.
- V_{rods} → The intersection volume of the rods with the triangle.

The second step is to calculate the surface area of the rods within the triangle area using the following equation (Li P. Y. et al., 2015: 6).

$$A_s = (3) \left(\frac{1}{6} \right) 2\pi r = \pi r \quad (31)$$

Where:

- A_s → The surface area of the rods

Finally, we can obtain the surface area to volume ratio by dividing **Equation 31** by **Equation 30**.

$$\frac{A_s}{V} = \frac{\pi r}{\frac{\sqrt{3}}{4} l^2 - \frac{1}{2} \pi r^2} \quad (32)$$

This example demonstrates the technical calculation for a single compression stage; it should be noted that implementing multiple compression stages increases the heat transfer, thus, improving the thermal efficiency (Li P. Y. et al., 2015: 6). For an Off-Shore wind turbine, it is recommended to use multiple compression stages, for the reason that they provide a higher surface area to volume ratio leading to an improvement in the heat transfer inside the chamber (Li P. Y. et al., 2015: 6).

A simulation for a traditional 220 MW CAES plant was conducted by the Iowa State University. The study involve a CAES system located in a wind farm for load levelling application and the porpose of the study is to demonstrate the benefits of a CAES system integrated within a wind farm, i.e., decrease the fluctuation of the electricity generation from wind turbines, and increase the load factor (*James D. & Das T., 2012*). The data used in the simulation is taken from the EWITS 2006 database (*EnerNex Corporation, 2011*). **Figure 33** shows the actual power generated by the wind turbines (P_a) and the forecasted scheduled power (P_{Sch}). The simulation was done using Matlab for the duration of one year (8760 hours). The mismatch between the actual power and the forcasted power is presented. The system functions as follows (*James D. & Das T., 2012: 16*):

- If $P_a > P_{Sch}$

Then the CAES system starts to store the surplus power generated from the wind turbines which is $P_a - P_{Sch}$

- If $P_a < P_{Sch}$

Then the CAES system starts to generate power which is $P_{Sch} - P_a$

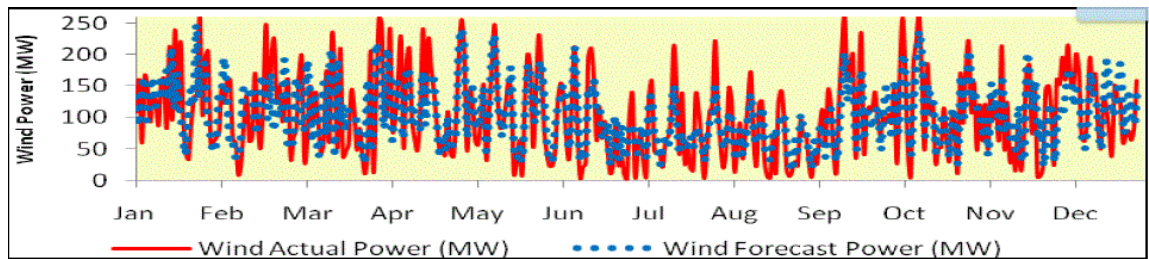


Figure 33: Mismatch between the actual and forecasted power from a wind farm (**James, D., 2012: 16**)

The CAES system is designed to have a 220 MW turbine and a 200 MW compressor, in addition, 150,000 m³ underground reservoir (*James, D., 2012: 16*). The charge ratio of the facility is 2:1, 8.629 hours to fully charge the storage system and 4.154 hours for discharging the system. The wind farm generates 188.12 GWh in a year and it needs additional 186.97 GWh to meet the forecasted power. With the help of the CAES system,

27.12% of the 188.12 *GW* is wasted and the rest is stored. 48.33% from the 186.97 *GW* is generated from the CEAS system and the rest is generated from external resources. Because 48.33% of the power needed to meet the scheduled, the facility saved 0.585 M\$ (James D. Das T., 2012: 18). A comparison of the impact of the system with and without CAES system when integrated with the wind farm is presented in **Table 11**.

Table 11: Impact of a CAES system in a wind farm (James D. & Das T., 2012: 19)

Operational factors	Without CAES	With CAES
<i>Demand supplied by a reserve (GW)</i>	186.97	96.6
<i>Carbon emissions (tons/year)</i>	62262	48527
<i>Carbon tax (M\$/year)</i>	2.262	1.765
<i>Capacity factor</i>	0.3644	0.4003

Due to the lack of data on the isothermal process, there is no information about I-CAES / Wind power hybrid system to be presented. Though, the positive impact on such a system could be assumed to be much higher than traditional CAES systems, for the reason that, no fossil fuel is needed, meaning, reduction on carbon emissions and operational cost without forgetting the increase in the efficiency of the system.

5. Economic Evaluation

I-CAES is a new technology that hasn't put its fingerprint on the energy market yet. As discussed earlier, LightSail Energy and SustainX demonstration projects have proved the technological potential for the I-CAES. Though, what is necessary for investors is, the economic feasibility of the technology. Different storage technologies could be valid for the same type of application; that is why an economic evaluation is necessary to determine the best technology based on its profitability.

5.1. Levelized Cost of Electricity (LCOE)

The Levelized Cost of Electricity (LCOE) is an economic assessment that facilitates the economic comparison between different technologies. It is calculated by dividing the total cost of the construction and operation of a plant over its lifetime by the total energy output over that lifetime. The LOCE represents the price of the technology per energy unit in the present money value (\$/kWh) (*Obi M. et al., 2016: 910*).

For storage systems, it is essential to distinguish between the capital cost of the power capacity and the capital cost of the energy capacity. The power capacity refers to the charging and discharging rated capabilities of a storage system. The Energy capacity refers to the size of the energy reservoir which is in this case, underground cavern or overground storage tanks (*Obi M. et al., 2016: 911*). The capital costs are incredibly vital for the calculation of LCOE. On the other hand, the O&M cost of the system consists of the cost of the energy used for the compression/expansion processes and the cost of the maintenance of the system.

Many parameters affect the LCOE of a storage facility such as efficiency, power, and energy capacity costs, buying and selling prices, capacity factor, and so forth. A sensitivity study was done for three CAES facilities (**Table 12**) by the Department of Electrical & Computer Engineering, Portland State University, USA. The goal of this study is to determine the most sensitive parameters affecting the LCOE of a facility. **Figure 34** shows the result of the study on McIntosh CAES plant (*Obi M. et al., 2016: 915*).

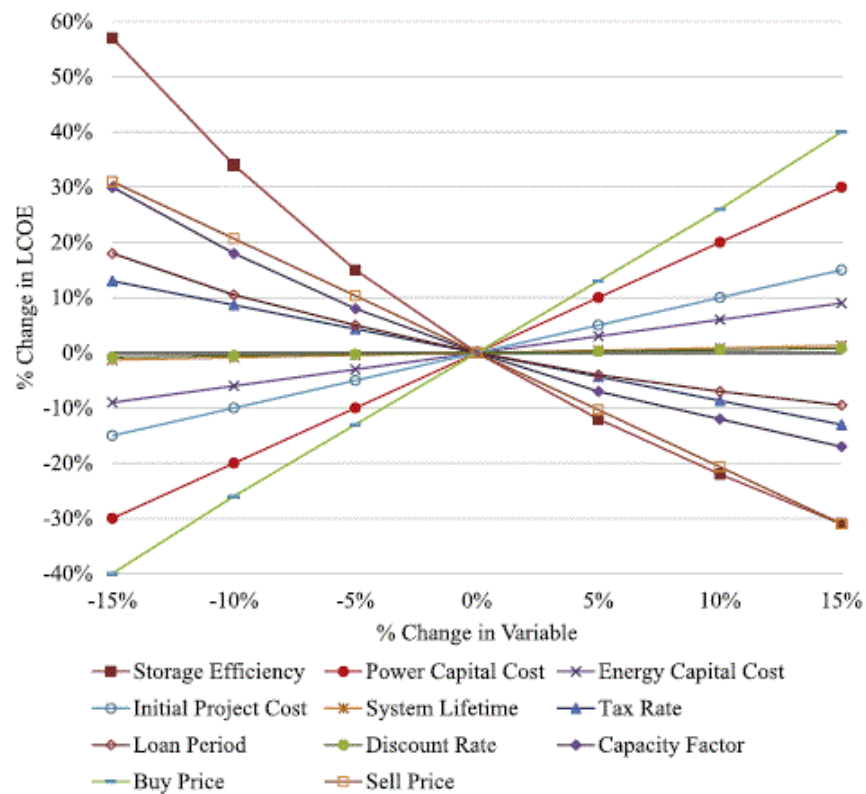


Figure 34: LCOE Sensitivity for NREL McIntosh CAES system (Source: Obi M. et al., 2016: 915)

Table 12: Sensitivity Analysis comparison of select three CAES technology cases (Source: Obi M. et al., 2016: 915)

EPRI 50 MW	SANDIA KERN 300 MW	NREL McIntosh
Capacity factor	Capacity factor	Storage efficiency
Project cost	Sell price	Buy price
Loan period	Storage efficiency	Capacity factor
Tax rate	Buy price	Sell price
Energy capital	Project cost	Project cost
Power capital	Loan period	Loan period

Also, the Monte Carlo technique was conducted during the study which is a technique that helps solve problems through computational algorithms (Kroese *P.*, 2011: 3). The technique was used to come up with the percentages of the parameters that most affect the LCOE, and the results were: storage efficiency (10%), Buy price (20%), Sell price (20%), Capacity factor (5%), Project cost (10%) (Obi *M. et al.*, 2016: 916).

5.2. CAES Cost

The capital costs of a CAES system, in general, consist of the expenses of the turbine, compressor, and the storage reservoir. The equation in which the cost of the system can be calculated is shown below (James *D. Das T.*, 2012: 13).

$$CAES_{cost} = P_T \times C_T \times P_C \times C_C \times E_{Rated} \times S_{Cap} \quad (33)$$

$$E_{Rated} = P_T \times T_{Discharge} \quad (34)$$

Where:

- $P_T \rightarrow$ Turbine power rating in MW
- $C_T \rightarrow$ Turbine cost in \$/kW
- $P_C \rightarrow$ Compressor power rating in MW
- $C_C \rightarrow$ Compressor cost in \$/kW
- $E_{Rated} \rightarrow$ Energy rating of CAES in kWh
- $S_{Cap} \rightarrow$ Cost of the storage capacity \$/kWh

Table 13 shows the cost breakdown for a CAES system in which the reservoir, turbine, and compressor have the dominant cost share among the subcomponents of a CAES system (84%) (IRENA, 2017: 57).

Table 13: CAES system cost breakdown for the year 2016 (Source: IRENA, 2017: 57)

Subcomponent	The share of cost (%), 2016
reservoir	40
Turbine	30
Compressor	14
Owner's cost	7
Balance of plant	6
Engineering, procurement, and construction management	3

5.3. Case Studies

The I-CAES technology is not yet public, meaning, it's not yet commercially available. For this reason, it is not possible to determine the capital costs of such a system due to the unavailability of a case study, i.e. procurement, labor, construction management, project management, engineering, and so forth. Currently, only estimations are available. Instead, case studies for traditional CAES systems are presented to examine the economic feasibility when integrated within a large scale RE systems. Given the available information on I-CAES, we will examine the economic feasibility of the technology when switching the traditional CAES system to an I-CAES system.

➤ CAES / Wind Farm

The Huntorf power plant is designed for a 290 MW power plant (Wang J., et al., 2017: 4). According to the information provided by the NREL, the power capacity cost for the system is 350 \$/kW and the energy capacity cost is 1.2 \$/kWh given the fact that, the reservoir can store up to 1227 MWh of energy, therefore the power and the energy capacity costs can be calculated as follow (Riaz M., 2010: 56):

$$\begin{aligned}
 P_{related\ cost} &= P_{cost} \times P_{capacity} \\
 &= 350 \frac{\$}{kW} \times 290,000\ kW = \$101,500,000
 \end{aligned}
 \tag{35}$$

$$\begin{aligned} E_{related\ cost} &= E_{cost} \times E_{capacity} \\ &= 1.2 \frac{\$}{kWh} \times 1227\ kWh = \$1,472,400 \end{aligned} \quad (36)$$

$$\begin{aligned} Capital\ cost &= P_{related\ cost} + E_{related\ cost} \\ &= \$101,500,000 + \$1,472,400 = \$102,972,400 \end{aligned} \quad (37)$$

As mentioned before, the operational costs consist of the cost of the energy bought for the compression/expansion processes and the cost of the maintenance of the system. Moreover, it is calculated using **Equation 38** (Riaz M., 2010). The Heat rate (H_R) is an index that reflects how efficient the facility is using the heat energy. In the Huntorf plant, the H_R is equal to 5563.98 Btu/kWh (Riaz M., 2010). The cost of fuel (natural gas) on a monthly basis is assumed to be 4.35 \$/MCF where 1 MCF = 1.026×10^6 Btu (Riaz M., 2010). That's mean, the monthly cost of natural gas for the plant is 4.24×10^{-6} \$/Btu. The Variable O&M cost assumed to be 5 \$/MWh (Riaz, M., 2010: 128).

$$\begin{aligned} Generation\ cost &= Fuel_{cost} \times H_R + O\&M_{cost} \\ &= 4.24 \times 10^{-6} \frac{\$}{Btu} \times 5563.98 \times 10^3 \frac{Btu}{MWh} + 5 \frac{\$}{MWh} \\ &= 28.59 \frac{\$}{MWh} \end{aligned} \quad (38)$$

The Iowa State University conducted a feasibility study to evaluate the economic potential for the D-CAES of Huntorf power plant when integrated to a wind farm with a generation capacity of 150 MW. The project's investment horizon assumed to be 40 years. The Locational Marginal Price (LMP) for the wind farm and the energy consumed by the D-CAES system on an hourly basis for three months (April, May, and June) are shown in **Figure 35 & 36** respectively.

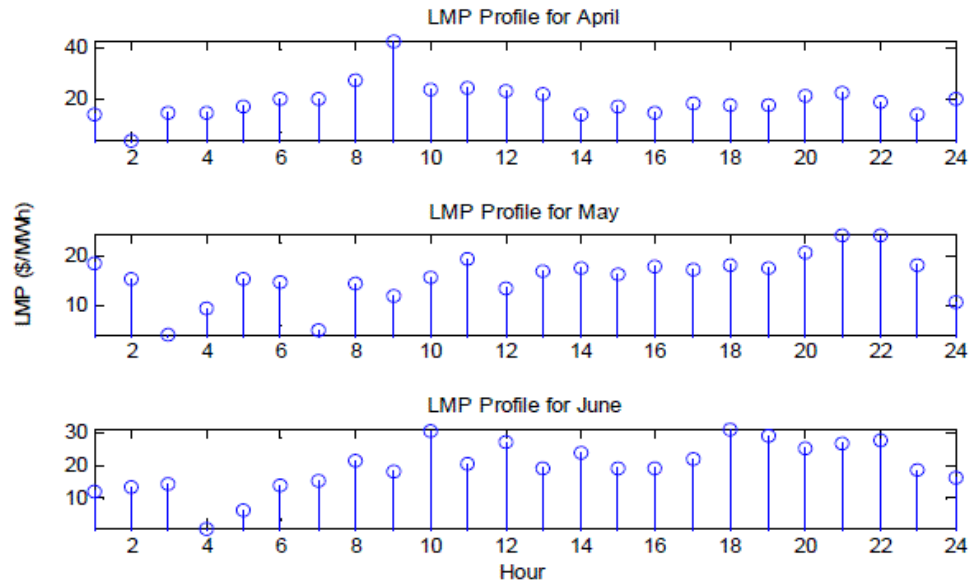


Figure 35: LMP simulation for 150 MW wind farm (Source: Riaz M., 2010: 127)

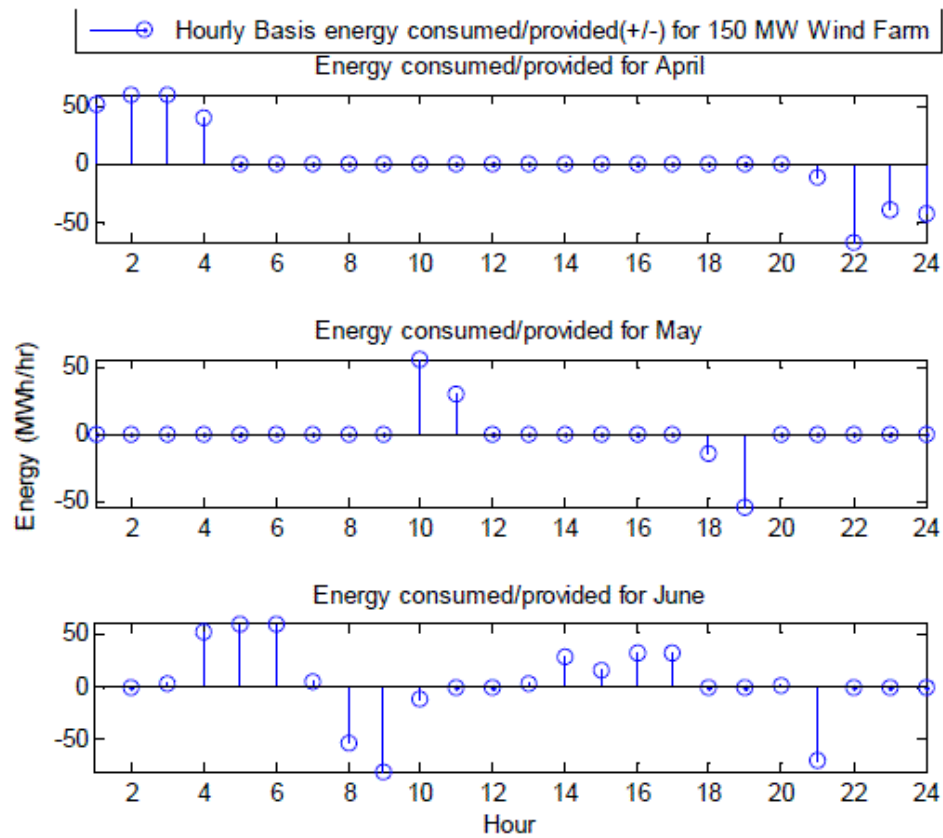


Figure 36: Energy consumed and generated by the D-CAES (Source: Riaz M., 2010: 128)

The revenue of the system can be expressed as follows (Riaz M., 2010: 130). Hence: results are shown in **Table 14**.

$$\begin{aligned}
 & \text{Revenue } (\$/\text{day}) \\
 &= \text{Discharging revenue } (\$/\text{day}) \\
 &\quad - \text{Charging cost } (\$/\text{day}) \\
 &\quad - \text{Cost of generation } (\$/\text{day})
 \end{aligned} \tag{39}$$

The D-CAES system is charged from the electricity produced from the wind farm. The charging cost of the system can be calculated by multiplying the amount of energy consumed by the LMP for each hour for the whole day (**Equation 40**) (Riaz M., 2010: 129). Hence: results are shown in **Table 14**.

$$\text{Charging cost } (\$/\text{day}) = \sum_{i=1}^{24} E_i(\text{MWh/hr}) \times \text{LMP}_i(\$/\text{MWh}) \tag{40}$$

Where:

- E_i is the amount of energy consumed for a specific hour.
- LMP_i is the Locational Margine Price for a specific hour.

The discharging revenue and the cost of generation for each hour can be calculated using **Equation 41 and 42** respectively (Riaz M., 2010: 130). Hence: results are shown in **Table 14**.

$$\begin{aligned}
 & \text{Discharging Revenue } (\$/\text{day}) \\
 &= \sum_{i=1}^{24} -E_i(\text{MWh/hr}) \times \text{LMP}_i(\$/\text{MWh})
 \end{aligned} \tag{41}$$

$$\begin{aligned}
 & \text{Cost of generation } (\$/\text{day}) \\
 &= \sum_{i=1}^{24} -E_i(\text{MWh/hr}) \times \text{Generation cost } (\$/\text{MWh})
 \end{aligned} \tag{42}$$

After that, to calculate the revenue per month, the revenue per day for a specific month is multiplied by the number of days in that month assuming the average daily output for the whole month (Riaz M., 2010: 130). Hence: results are shown in **Table 14**.

$$\begin{aligned}
 & \text{Month}_i \text{ revenue} \\
 &= \text{Revenue per day for month}_i \\
 &\times \# \text{ of days in month}_i
 \end{aligned}
 \tag{43}$$

Table 14 shows the cash flow of the hybrid system, i.e. the D-CAES system and the 150 MW wind farm for a whole year.

Table 14: D-CAES/Wind farm system cash flow (Source: Riaz M., 2010: 131)

Month	Charging cost (\$/day)	Generation cost (\$/day)	Discharge revenue (\$/day)	Revenue (\$/day)	Revenue (\$/month)
January	5724.496	5081.87	4885.57	-5920.79	-183,545
February	842.7684	1445.28	1060.82	-1227.23	-34,362.4
March	1528.3064	3816.79	2855.98	-2489.11	-77,162.6
April	2414.5499	4560.96	2939.62	-4035.89	-121,077
May	1460.9927	1930.96	1191.30	-2200.66	-68,220.4
June	3669.03488	6095.67	4777.77	-4986.93	-149,608

July	2995.1744	4321.6	2509.91	-4806.92	-149,015
August	336.49121	297.32	250.45	-383.353	-11,883.9
September	2447.6357	4323.66	2905.19	-3866.1	-115,983
October	2565.7042	3053.15	2696.46	-2922.4	-90,594.3
November	1304.2962	1476.38	461.41	-2319.27	-69,578.2
December	4547.1766	4588.98	7664.00	-1472.16	-45,636.9
Total					-\$1,116,667

As we can see in **Table 14**, the revenue for each month is negative; this means that the project is losing money every month for the whole year.

The net present value (NPV) shows whether the project is profitable or not by calculating how much money the project will make or loss during the investment horizon, and it can be calculated using **Equation 44** (Juhász L., 2011: 47).

$$\begin{aligned}
 NPV &= CF_0 \sum_{t=1}^n \frac{CF_t}{(1 + IRR)^t} \\
 &= -102,972,400 + \sum_{t=1}^{40} \frac{-1,116,667}{(1 - 0.01)^t} = -148,090,258
 \end{aligned}
 \tag{44}$$

Where:

- CF_0 is the capital investment
- CF_t is the annual return
- IRR is the internal rate of return which is usually used to estimate the profitability of a project.
- NPV is the net present value

The IRR indicates the rate in which the project is earning or losing money, and it is equal to -1% which mean that the project is losing money. The IRR was calculated as follow: (Juhász L., 2011: 47).

$$\begin{aligned} IRR &= \frac{\text{Annual return}}{\text{Capital investment}} \\ &= \frac{-1,116,667}{102,972,400} = -0.01 = -1\% \end{aligned} \quad (45)$$

This case study demonstrates that the integration of low efficient D-CAES within a large RE system is not economically feasible. From the sensitivity study presented in **Table 12**, we know that the buying price of electricity affects the LCOE dramatically and the buying price, in this case, is higher than the selling price leading to a negative NPV which mean that the hybrid system is not economically feasible. The solution to this problem is to make the whole system generate energy from renewable sources. That is why the I-CAES is a promising technology. Switching from a D-CAES system to an efficient I-CAES system will eliminate the use of fossil fuels and reduce the required energy for the operation process of the system leading to a significant reduction in the power cost.

➤ CAES / PV / Grid

PV technologies still straining to overcome the challenge that prevents it to be reliable to end users, i.e. the dependency of the intermittent source. The solar radiation from the sun varies from hour to hour leading to a variation in the voltage and the energy generated by the system. For this reason, a PV system needs a voltage regulator and a backup power system to meet the demand. Another solution to the problem is a storage system.

The CAES technology has the potential to smooth out the variation of the energy generated by the PV system; it also can be used in a time-shift application by storing the energy at daytime when the demand is low and produce it at evening hours when the demand is high. The Arizona Research Institute for Solar Energy (AzRISE) conducted a study to see the economic impact of three different scenarios for electricity generation; the scenarios are as follow: (AzRISE, 2010: 43).

- 1) Grid + PV
- 2) Grid + CAES
- 3) Grid + CAES + PV

The following are the assumptions made for the study: (AzRISE, 2010: 43).

- The PV system has a capacity of 100 MW
- 13 hours generation capacity from the CAES system
- 200 MW compressor capacity
- 135 MW generation capacity
- Price of natural gas: 37.8 \$/MWh
- The CAES requires 0.75 kWh to generate 1 kWh

PV + Grid → It is assumed that the operator of the PV system forecasted the energy generation from the PV system for each hour of the day to sell it to the grid, this forecast is of course subjected to an error.

The costs of the PV/CAES hybrid system for this case study is shown in **Table 15** (AzRISE, 2010: 43).

Table 15: Cost of PV / CAES hybrid system (Source: AzRISE, 2010: 45)

<i>Item</i>	<i>Cost per unit</i>
<i>Capital costs</i>	
<i>PV modules, Invertors, and installation</i>	<i>5,040 \$/kW</i>

<i>PV Inverter Replacements</i>	<i>756 \$/kW</i>
<i>CAES generator</i>	<i>190 \$/kW</i>
<i>CAES Compressor</i>	<i>175 \$/kW</i>
<i>CAES Balance of Plant</i>	<i>230 \$/kW</i>
<i>CAES Reservoir</i>	<i>2 \$/kWh</i>
<i>Performance Assumptions & Operational Costs</i>	
<i>PV fixed O&M</i>	<i>20.9 \$/kW</i>
<i>PV degradation rate / year</i>	<i>1%</i>
<i>CAES H_R</i>	<i>4,300 Btu/kWh</i>
<i>CAES fixed O&M</i>	<i>3.69 \$/kW</i>
<i>CAES variable O&M</i>	<i>0.006 \$/kW</i>
<i>Financial Assumptions</i>	
<i>Interest Rate</i>	<i>6%</i>
<i>CAES tax and insurance</i>	<i>1.5% of the capital investment</i>
<i>PV tax and insurance</i>	<i>1% of the capital investment</i>

According to the study, the average daily revenue is \$ 34,031; after that, the revenue decreases every year due to the 1% PV degradation rate per year (AzRISE, 2010: 43).

CAES + Grid → During low demand hour and high electricity generation; the grid sends the surplus energy to the CAES system to store the energy for the time of high demand. The selling and the storing time for each hour during the day for the whole year are calculated using programming algorithm, i.e., MATLAB, the reason for that is to avoid the extra charging cost of the system when unnecessary. The average revenue per day for the CAES + Grid system is \$30,040 (AzRISE, 2010: 46).

PV + CAES + Grid → in this system, the CAES receive the energy from both the grid and the PV system to store it and reproduce it during high demand hours. The average daily revenue for the system is \$-64,071 (AzRISE, 2010: 46). The NPV for the daily arbitrage models for all the three scenarios are presented in **Table 16** below.

Table 16: Daily arbitrage & NPV for three different scenarios (all costs are in \$ millions)
(Source: AzRISE, 2010: 47)

	<i>PV + Grid</i>	<i>CAES + Grid</i>	<i>PV + CAES + Grid</i>
Net revenue (NR)	\$145.4	\$140.3	\$285.7
Costs			
PV capital	\$576.8		\$576.8
PV O&M Tax & Insurance	\$91.1		\$91.1
CAES generation		\$25.7	\$25.7
CAES compressor		\$35	\$35
CAES other		\$111.5	\$111.5
CAES O&M Tax & insurance		\$37.7	\$37.7
Total Cost (TC)	\$667.9	\$209.9	\$887.8

Subsidies			
Total subsidies (TS)	\$553		\$553
NPV			
Total NPV	\$30.5	-\$69.6	-\$39.1

The CAES + Grid and the PV + CAES + Grid scenarios show a negative NPV.

$$\begin{aligned}
 NPV_{CAES+Grid} &= NR - TC \\
 &= \$140.3 - \$209.9 = -\$69.6
 \end{aligned}
 \tag{46}$$

$$\begin{aligned}
 NPV_{PV+CAES+Grid} &= NR - (TC - TS) \\
 &= \$285.7 - (\$887.8 - \$553) = -\$39.1
 \end{aligned}
 \tag{47}$$

As before mentioned, the traditional CAES system requires 0.75 kWh to generate 1 kWh , this means that the system has a low round-trip efficiency. It also has a high generation cost because of the need of the natural gas for adding heat to the compressed air during the expansion process. Moreover, the system has a capacity of 135 MW which means that the cost associated with the combustion of fossil fuel is:

$$= 135 \text{ MW} \times 37.8 \frac{\$}{\text{MW}} = \$5,103
 \tag{48}$$

According to the study conducted by AzRISE, if the CAES system reduces the required energy for operating from 0.75 kWh to 0.6 kWh , the system would have a positive NPV of \$ 22.3 millions (AzRISE, 2010: 47) which is possible by using an I-CAES system.

The use of an I-CAES eliminates the need of natural gas and reduce the amount of energy required for the operation process due to its high round-trip efficiency ($\cong 80\%$) leading to a reduction in the power capacity cost.

5.4. Economic of I-CAES

The economic evaluation for a CAES technology varies between small and large scale systems. **Table 17** shows the financial situation of large and small scale CAES systems.

Table 17: Economic comparison between large and small scale CAES system (Luo X. et al., 2014: 607)

Size	Power capital cost (\$/kW)	Energy capital cost (\$/kWh)	O&M cost (\$/kWh)
Large-CAES	~400 – 1000	2 – 120	0.003
Small-CAES	~500 – 1500	200 - 250	Very low

The traditional CAES systems are not economically feasible for small-scale applications because it has a low-trip efficiency and requires high capital costs (**see Table 14**), this means that if the application needs a small amount of energy, the revenue would be minimal compared to the investment cost. The I-CAES is not commercially available at this moment, but few demonstration projects have been done by companies such as SustainX and LightSail to prove the economic feasibility of an I-CAES system for small and large scale applications.

As shown in **Table 13**, the reservoir of the storage system contributes significantly to the cost of a CAES system (40%). The Lightsail company came up with a solution to overcome this challenge for small-scale applications which is, using a cheap spun carbon-fiber overground tanks as shown in **Figure 21**.

Also, SustainX went through three major steps for developing a highly efficient and low-cost I-CAES, 1 kW prototype, 40 kW system, and the final one 1.5 MW system. The 1.5 MW system is in operation since 2014; the project cost was \$ 13,046,588 (Liu X. et al.,

2017: 17). Though, the cost of such a system is much less than this number. The cost of the system was high because it's the first MW system so, the company conducted many types of research and experiments where they had to build machines for experimental reasons before making the actual 1.5 MW I-CAES system, but now since they have the know-how, the construction of such a system will cost much less.

The Energy Storage Association says “The technology compresses and expands gas near-isothermally over a wide pressure range, namely from atmospheric pressure (0 psig) to a maximum of about 2,500 psig. This large operating pressure range, along with the isothermal gas expansion (allowing for recovery of heat not achieved with adiabatic expansion), achieves a ~7x reduction in storage cost as compared to traditional CAES in vessels” (ESA, 2018).

Currently, the estimated for an I-CAES system is 2400 – 3000 \$/kW, or 400 – 500 \$/kWh (EPRI, 2015: 2). Though, the fixed and variable O&M cost of I-CAES system is expected to be higher due to the complexity of the system to achieve higher overall efficiency (Aquino, T., 2017: 47).

Table 18: Economic comparison between I-CAES system from SustainX and LightSail (Source: EPRI, 2015: 2)

	<i>SustainX</i>	<i>LightSail</i>
<i>Vendor Cost Expectation</i>	<i>\$2,400-3,000/kW (\$400-500/kWh) for turnkey 6-hour at production volume</i>	<i>\$500/kW (\$100/kWh)</i>

Table 19 shows an economic comparison for large and small scale systems between D-CAES and I-CAES systems. It is clear that for small-scale system I-CAES is better than D-CAES system for several reasons such as:

- The use of an isothermal process in the CAES technology eliminates the need for fossil fuels leading to a reduction in the generation cost.
- The use of small overground storage tanks as a storage facility instead of underground caverns.

Although small overground storage tanks for small-scale applications is economically reasonable, big overground storage tanks for large-scale applications is not. As shown in **Table 20**, the cost of energy storage components for an overground storage reservoir (i.e., surface piping) is 30 times higher than an underground salt caverns. The total cost of the underground reservoir is less than an overground storage reservoir though, there are no small size underground caverns, which means, for small-scale applications, underground caverns are not economically feasible because the investor will end up spending extra money in a space that will not be used.

Table 19: Economic comparison for large/small scale systems between D-CAES & I-CAES systems (Source: EPRI (2015: 2) & Luo X. (2014: 607))

Scale size	D-CAES		I_CAES	
	Power capital cost (\$/kW)	Energy capital cost (\$/kWh)	Power capital cost (\$/kW)	Energy capital cost (\$/kWh)
Large-scale	~400 – 1000	2 – 120	\$2,400 - 3,000/kW	\$400-500/kWh
Small-scale	~500 – 1500	200 - 250	\$500/kW	\$100/kWh

Table 20: Economic comparison between underground and overground storage facilities (Source: Wang J. et al., 2017: 5)

Reservoir	Size (MWe)	CPRC (\$/kW)	CESC (\$/kWh)	ST (hours)	TC (\$/kWe)
Underground (Salt caverns)	200	350	1	10	360
Overground (Surface piping)	20	350	30	3	440

Where:

- CPRC → The cost for Power-Related Components
- CESC → The cost for the Energy Storage Components
- ST → The storage duration in hours
- TC → Total cost

6. Conclusion

ESS, in general, have the potential to solve many problems that the energy market is facing. For an instant, it has the potential to change the world's electric grid and cause a monumental shift from the dependency on fossil fuel to renewable sources, and decentralize the grid. These changes will drive the world to decarbonize through the deployment of RE systems.

Another problem that ESS could solve is, the lack of electric grids in some rural areas where the support of off-grid applications that ESS can offer has the potential to mitigate poverty and improve people's living conditions. However, to achieve these goals, we need ESS that can function in reliable and cost-effective manners for large, medium, and small-scale applications. Many ESS technologies can offer to support different type of applications. In this paper, we focused on the CAES system in general and on I-CAES system in specific. Traditional CAES systems with its low round-trip efficiency showed the potential to support large-scale applications when integrated with fossil fuel-based plants, e.g., Huntorf and McIntosh plants. Though, the technology still has enormous potential when it comes to energy savings possibilities; these possibilities include energy recovery through capturing heat, pressure reduction, improve isolation, the right choice of compressor size, and optimization of the operation process. The road to a cost-effective, efficient and environmentally friendly CAES system began beforehand with I-CAES system. As aforementioned, there is no existed I-CAES system yet, but the technology already proved its technological and cost-effectiveness with the demonstration project conducted by SustainX and LightSail companies. It has the potential to eliminate the geographical constraints linked to the technology and save a tremendous amount of cost by using overground storage tanks instead of underground caverns that contributes to 40% of the total cost of the system. It also reduces the energy generation cost by reducing the amount of energy it needs to function by improving the overall system efficiency that reaches 80%. Nevertheless, the I-CAES system proved its potential for small-scale applications which is suitable for off and smart-grid applications. The technology still needs some innovation and improvements to make it able to support large-scale applications, for the reason that, large-scale overground storage tanks are expensive, and when using such storage tanks, the system will not be economically feasible.

Bibliography

- [1] Al-Shemmeri T. (2010): Engineering Thermodynamics. bookboon
- [2] Aquino T. / Zuelch C. / Koss C. (2017): Energy Storage Technology Assessment. HDR, New Mexico
- [3] AzRISE (2010): Study of Compressed Air Energy Storage with Grid and Photovoltaic Energy Generation. AzRISE, Arizona
- [4] Boveri & CIE. (1978): Energy Supply, Federal Republic of Germany. Mannheim
- [5] bp. (2017): BP Statistical Review of World Energy. 66th ed., Forest For All Forever, London
- [6] Brian E. & Brix W. M. (2011): Efficiency of Compressed Air Energy Storage. Technical University of Denmark, Lyngby
- [7] Chen H. / Zhang X. / Liu J. / Tan C. (2013): Compressed Air Energy Storage. In: Energy Storage - Technologies and Applications. pp. 101-110, INTECH, Beijing
- [8] EPRI. (2015): Technology Briefing: Near-Isothermal CAES. <https://www.epri.com/#/pages/product/000000003002003359/?lang=en> retrieved on Jan 26, 2015
- [9] ESA. (2018): Isothermal CAES. <http://energystorage.org/energy-storage/technologies/isothermal-caes> retrieved in 2018
- [10] EnerNex Corporation. (2011): EASTERN WIND INTEGRATION AND TRANSMISSION STUDY. University of North Texas Libraries, Colorado
- [11] EPRI. (2014). NYPA Completes Design, Performance and Thermodynamic Studies. [file:///C:/Users/hp/Downloads/000000003002001483%20\(2\).pdf](file:///C:/Users/hp/Downloads/000000003002001483%20(2).pdf) retrieved in Jan 2014
- [12] Fidalgo J. & Rañal F. (2014): Physic and Chemistry. 3rd ed., DM, Santiago de Compostela
- [13] Garvey S. D. & Pimm A. (2016): Compressed Air Energy Storage. In: Storing Energy. pp. 87-111, Elsevier, Durban
- [14] Heidari M. / Mortazavi M. / Rufer A. (2017): Design, modeling and experimental validation of a novel finned reciprocating compressor for Isothermal Compressed Air Energy Storage applications. In: Energy. pp. 1252-1266, Elsevier, Lausanne
- [15] IEA. (2014): Technology Roadmap - Energy storage, IEA, Paris

- [16] IEC. (2011): Electrical Energy Storage. IEC, Geneva.
- [17] IEA. (2007): Contribution of Renewable Energy to Energy Security. OECD/IEA, Paris
- [18] IRENA. (2017): ELECTRICITY STORAGE AND RENEWABLES: COSTS AND MARKETS TO 2030. IRENA, Abu Dhabi
- [19] IRENA. (2018): OFF-GRID RENEWABLE ENERGY SOLUTIONS. IRENA, Abu Dhabi
- [20] James D. & Das T. (2012): Compressed Air Energy Storage. Iowa State University, Iowa
- [21] Juhász L., (2011): NET PRESENT VALUE VERSUS INTERNAL RATE OF RETURN. In: Economics & Sociology. 4 (1), pp. 46-53.
- [22] Kroese P. (2011): Monte Carlo Methods. AMSI, Queensland
- [23] Kim M. Y. (2012): Novel concepts of compressed air energy storage and thermo-electric energy storage. Ph.D. thesis, ÉCOLE POLYTECHNIQUE FÉDÉRALE DE LAUSANNE, Lausanne
- [24] Liu X. / Marnay C. / Feng W. / Zhou N. / Karali N. (2017): A Review of the American Recovery and Reinvestment Act Smart Grid Projects and Their Implications for China. LBNL, California
- [25] Li P. Y. / Loth E. / Simon Terrence W. / Van de Ven James D. / Crane Stephen E. (2015): Compressed Air Energy Storage for Offshore Wind Turbines, ResearchGate
- [26] Luo X. & Wang J. (2013): OVERVIEW OF CURRENT DEVELOPMENT ON COMPRESSED AIR ENERGY STORAGE. EERA, Coventry
- [27] Luo X. / Wang J. / Dooner M. / Clarke J. / Krupke C. (2014): Overview of current development in compressed air energy storage technology. In: Energy Procedia. 62 (1), pp. 603-611.
- [28] McConnaughey T. B. / Young C. / McFarland E. (n.d): TECHNO-ECONOMIC EVALUATION OF COMPRESSED AIR ENERGY STORAGE IN UNCONVENTIONAL APPLICATIONS. The University of Queensland, Brisbane
- [29] Muñoz S. A. / Garcia M. / Gerlich M. (2016): Overview of storage technologies. Sensible

- [30] Obi M. / Jensen S. M. / Ferris Jennifer B. / Bass Robert B. (2016): Calculation of levelized costs of electricity for various electrical energy storage systems. In: Renewable and Sustainable Energy Review. 67 (1), pp. 908-920
- [31] Riaz M. (2010): Feasibility of compressed air energy storage to store wind on monthly and daily basis. Graduate Theses and Dissertations, Iowa State University, Iowa
- [32] Raible M. (2016): Study of Compressed Air Energy Storage (CAES) for Domestic Photovoltaic Systems. Master thesis, Instituto Politécnico de Setúbal, Escola Superior de Tecnologia de Setúbal, Setúbal
- [33] Reitz R. D. (1996): Computer Modeling of Sprays. University of Wisconsin, Pittsburgh
- [34] RWE Power AG (2010): ADELE – ADIABATIC COMPRESSED-AIR ENERGY STORAGE FOR ELECTRICITY SUPPLY. RWE, Essen.
- [35] Raju M. & Kumar K. S. (2012): Modeling and simulation of compressed air storage in caverns: A case study of the Huntorf plant. In: Applied Energy, 89 (1), pp. 474-481
- [36] Stoppato A. & Benato A. (2017): The Importance of Energy Storage. In: Energy Storage. pp. 1-26, Padua University, Padua
- [37] Susan M. / Schoenung J. / Hassenzahl W. V. (2003): Long- vs. Short-Term Energy Storage Technologies Analysis. Sandia National Laboratories, California
- [38] SustainX (2015): Demonstration of Isothermal Compressed Air Energy Storage to Support Renewable Energy Production. SustainX, California
- [39] Taranovich S. (2012): Regenerative air energy storage.
<https://www.edn.com/electronics-blogs/powersource/4395690/Regenerative-air-energy-storage> retrieved on Sep 8, 2012
- [40] Taylor D. A. (1996): Introduction to Marine Engineering. (2nd ed.), Elsevier
- [41] The Federal Ministry for Economic Affairs and Energy. (2015): The Energy of the Future. Federal Ministry for Economic Affairs and Energy Public Relations, Munich
- [42] U.S. Department of Energy (2008): 20% Wind Energy by 2030. U.S. Department of Energy, Virginia
- [43] Villela D. / Kasinathan V. V. / De Valle S. / Alvarez M / Frantziskonis G. / Frantziskonis P. / Muralidharan K. (2010): COMPRESSED-AIR ENERGY STORAGE SYSTEMS FOR STAND-ALONE OFF-GRID PHOTOVOLTAIC MODULES. University of Arizona, Arizona

- [44] Wang J. / Lu K. / Ma L. / Wang J. / Dooner M. / Miao S. / Li J. / Wang D.
(2017): Current research and development trend of compressed air energy storage.
In: *Energies*. 10 (7), pp. 434–448.

Abbreviation

A-CAES	<i>Adiabatic Compressed Air Energy Storage</i>
ADELE	<i>Adiabatic Compressed Air Energy Storage for Electricity Supply</i>
AZRISE	<i>The Arizona Research Institute for Solar Energy</i>
ASME	<i>American Society of Mechanical Engineers</i>
Bp	<i>British Petroleum Company</i>
CAES	<i>Compresses Air Energy Storage</i>
CO₂	<i>Carbon dioxide</i>
D-CAES	<i>Diabatic Compressed Air Energy Storage</i>
EES	<i>Energy Storage System</i>
EASE	<i>European Association for Storage of Energy</i>
GHG	<i>Greenhouse gases</i>
HPLIA	<i>High-Pressure, Liquid-in-Air machine</i>
I-CAES	<i>Isothermal Compresses Air Energy Storage</i>
ISO	<i>The International Organization for Standardization</i>
IEC	<i>International Electrotechnical Commission</i>
IRR	<i>Internal Rate of Return</i>
IRENA	<i>International Renewable Energy Agency</i>
LCOE	<i>Levelized Cost of Electricity</i>
Li-ion	<i>lithium-ion</i>
LMP	<i>Locational Marginal Price</i>

<i>MW</i>	<i>Megawatt</i>
<i>MWh</i>	<i>Megawatt-hour</i>
<i>kWh</i>	<i>Kilowatt-hour</i>
<i>NPV</i>	<i>Net Present Value</i>
<i>NREL</i>	<i>National Renewable Energy Laboratory</i>
<i>O&M</i>	<i>Operation and Maintenance</i>
<i>PV</i>	<i>Photovoltaic</i>
<i>PHS</i>	<i>Pumped Hydroelectric Storage</i>
<i>psig</i>	<i>pounds per square inch gauge</i>
<i>psia</i>	<i>Pound-force per square inch Absolute</i>
<i>psid</i>	<i>pounds per square inch differential</i>
<i>RE</i>	<i>Renewable Energy</i>
<i>RES</i>	<i>Renewable Energy Sources</i>
<i>RPM</i>	<i>Revolution per minute</i>
<i>RWE</i>	<i>Rheinisch-Westfälisches Elektrizitätswerk</i>
<i>SMES</i>	<i>Superconducting magnetic energy storage</i>
<i>T&D</i>	<i>Transmission and Distribution</i>
<i>TES</i>	<i>Thermal Energy Storage</i>
<i>U.S</i>	<i>United States</i>
<i>UNIDO</i>	<i>United Nations Industrial Development Organization</i>
<i>USD</i>	<i>United States Dollar</i>

List of Figures

Figure 1: Problems with RE installation and possible solutions (Source: IEC, 2011: 12)	6
Figure 2: Energy storage technologies categorized according to available power and typical charge/discharge timescale, including several proposed applications (Source: Muñoz S. A. et al., 2016: 28)	9
Figure 3: Comparison of power density and energy density for different ESS technologies (Source: Muñoz S. A. et al., 2016: 24)	9
Figure 4: ESS technologies categorized according to the type of application areas based on power rating and rated energy capacity (Source: Muñoz S. A. et al., 2016: 23)	10
Figure 5: Investment cost of ESS technologies (Source: Muñoz S. A. et al., 2016: 25)	11
Figure 6: D-CAES system (Source: Garvey S. D. & Pimm A., 2016: 103).....	13
Figure 7: D-CAES system with recuperator (Source: Garvey S. D. & Pimm A., 2016: 103)	14
Figure 8: D-CAES system with recuperator and two expansion stages (Source: Garvey S. D. & Pimm A., 2016: 104).....	14
Figure 9: Temperature/Pressure plot of D-CAES with three compression stages and two expansion stages and recuperator (Source: Garvey S. D. & Pimm A., 2016: 104)	15
Figure 10: A-CAES with thermal storage (Source: Garvey S. D. & Pimm A., 2016: 106)	16
Figure 11: Huntorf Power plant (Source: Boveri & CIE, 1978: 5).....	19
Figure 12: Operating Data of Huntorf Storage System (Source: Boveri & CIE, 1978: 9)	19
Figure 13: McIntosh power plant (Brian E. & Brix W. M., 2011: 7).....	21
Figure 14: A-CAES plant - ADELE (Source: RWE Power AG, 2010: 5)	22
Figure 15: P-V diagram for CAES system (Source: Heidari M. et al., 2017: 1253)	23

Figure 16: heat transfer rate and work change with the polytropic factor (Source: Heidari M. et al., 2017: 1254).....	24
Figure 17: P-V diagram for the isothermal process (Source: Fidalgo J. & Rañal F., 2014: 39)	26
Figure 18: I-CAES LightSail Company's Approach (Taranovich S., 2012).....	29
Figure 19: LightSail modified reciprocating compressor (Source: EPRI, 2015: 2).....	30
Figure 20: Illustration of the reversible process of I-CAES system from LightSail Company (Source: Taranovich S., 2012)	31
Figure 21: Low-cost storage containers within a shipping container (Source: Taranovich S., 2012).	32
Figure 22: SustainX compression/expansion of the marine diesel reciprocating engine and an illustration for the storage reservoir (EPRI, 2014: 5).....	33
Figure 24: Energy/Exergy flow of the I-CAES system (Source: Kim M. Y., 2012: 22) ..	39
Figure 25: HPLIA Machine for testing spraying water under different conditions (Source: SustainX, 2015: 19).....	41
Figure 26: Heat-transfer test stand (HXTST) and Experimental results (Source: SustainX, 2015: 20)	42
Figure 27: Population served by off-grid RS technologies in Africa (Source: IRENA, 2018: 4)	44
Figure 28: A simplified illustration of the liquid piston (Taylor D. A., 1996: 115)	45
Figure 29: The compressor developed prototype (Source: Villela D. et al., 2010: 4) ...	46
Figure 30: The system efficiency as a function of the compression rate (rpm) (Source: Villela D. et al., 2010: 5).....	46
Figure 31: CAES/Wind turbine hybrid system (Source: Li P. Y. et al., 2015: 4)	48
Figure 32: The liquid piston chamber (Source: Li P. Y. et al., 2015: 4).....	48
Figure 33: Rods inside the liquid piston chamber (Source: Li P. Y. et al., 2015: 6).....	50
Figure 34: Mismatch between the actual and forecasted power from a wind farm (James, D., 2012: 16)	52

Figure 35: LCOE Sensitivity for NREL McIntosh CAES system (Source: Obi M. et al., 2016: 915)	55
Figure 36: LMP simulation for 150 MW wind farm (Source: Riaz M., 2010: 127).....	59
Figure 37: Energy consumed and generated by the D-CAES (Source: Riaz M., 2010: 128)	59

List of Tables

Table 1: Characteristics of ESSs for typical applications in the energy system (Source: IEA, 2014: 9).....	7
Table 2: Main characteristics of ESSs (Source: Wang J. et al., 2017: 2)	8
Table 3: Application category and its specifications (Source: Susan M. et al., 2003: 11)	10
Table 4: ESS technologies for long and short term applications (Source: IEA, 2014: 18)	12
Table 5: D-CAES key performance data (Source: EASE, 2018).....	15
Table 6: A-CAES key performance data (Source: EASE, 2018).....	17
Table 7: Key features - Huntorf and McIntosh CEAS plants (Source: Wang J. et al., 2017: 10)	18
Table 8: Operating conditions for the Huntorf plant (Source: Raju M. & Kumar K. S., 2012: 476)	20
Table 9: Quantities of air can be compressed with 1 kWh of work (Source: Gavery S. D. & Pimm A., 2016: 93).....	28
Table 10: LightSail's Experimental Efficiency Result for the I-CAES system (Source: Taranovich S., 2012)	31
Table 11: Impact of a CAES system in a wind farm (James D. & Das T., 2012: 19)	53
Table 12: Sensitivity Analysis comparison of select three CAES technology cases (Source: Obi M. et al., 2016: 915)	55
Table 13: CAES system cost breakdown for the year 2016 (Source: IRENA, 2017: 57)	57
Table 14: D-CAES/Wind farm system cash flow (Source: Riaz M., 2010: 131).....	61
Table 15: Cost of PV / CAES hybrid system (Source: AzRISE, 2010: 45)	64
Table 16: Daily arbitrage & NPV for three different scenarios (all costs are in \$ millions) (Source: AzRISE, 2010: 47).....	66

Table 17: <i>Economic comparison between large and small scale CAES system (Luo X. et al., 2014: 607).....</i>	68
Table 18: <i>Economic comparison between I-CAES system from SustainX and LightSail (Source: EPRI, 2015: 2).....</i>	69
Table 19: <i>Economic comparison for large/small scale systems between D-CAES & I-CAES systems (Source: EPRI (2015: 2) & Luo X. (2014: 607))</i>	70
Table 20: <i>Economic comparison between underground and overground storage facilities (Source: Wang J. et al., 2017: 5).....</i>	70